Iranian Journal of Fuzzy Systems

Volume *, Number *, (****), pp. **

Original paper

Resilient finite-time extended passive filtering for switched fuzzy systems with cyber-attacks

S. P. Sathiyapriya [1]

[1] *Department of Mathematics, Kumaraguru College of Technology, Coimbatore-641049, Tamil Nadu, India.*

sathisp2.maca@gmail.com

Abstract

This article focuses on developing a robust resilient filtering approach for discrete-time switched fuzzy systems subject to random gain fluctuations and sensor malfunctions. In this framework, sensor outputs are modeled as stochastic processes that operate under varying failure probabilities. The addressed system dynamics also incorporate gain variations characterized by Bernoulli-distributed white noise sequences. With the aid of an appropriately formulated Lyapunov functional and finite-time stability theory, new sufficient conditions are derived in the form of linear matrix inequalities, ensuring that the enhanced fuzzy system achieves stochastic finite-time boundedness along with the desired passivity extension. Moreover, the proposed framework provides a systematic way to handle uncertainties and disturbances in practical control environments. To demonstrate the practical effectiveness of the proposed filter design, three numerical examples are presented, including cases drawn from robotic arm dynamics and nonlinear electronic circuits.

Keywords: Takagi-Sugeno fuzzy model, switched systems, extended passive filter, finite-time analysis, cyber-attacks, non-fragile filtering, randomly occurring gain variation, average dwell-time.

1 Introduction

Switched systems represent an important class of hybrid systems. They are widely used to model complex dynamics in physical engineering domains such as electronics, mechanical systems, power systems, chemical processes, air traffic control and aircraft systems [3, 11]. In particular, switched systems can be characterized by a collection of discrete-time or continuous-time subsystems, along with a switching rule that governs the transitions between these subsystems. Switched systems uncover wide-ranging applications across multiple engineering domains and have gained substantial significance lately. Some notable applications for switched systems are automotive industry, transmission and stepper motors and switching power converters [9, 26]. As a representative category of constrained switching signals, average dwell-time switching encompasses dwell-time switching, with its extreme manifestation being the arbitrary switching. Hence, exploring the stability analysis and control of switched systems using the average dwell-time technique holds both, practical and theoretical consideration. In [12], the authors tackled the problem of achieving switched linear time-delay systems utilizing finite-time stabilization by means of saturating actuators.

From a practical standpoint, the theoretical framework developed in this study finds essential deployment in complex, high-reliability engineering environments such as networked robotic manufacturing cells, smart grid distribution systems, and autonomous transport architectures. In these real-world setups, state measurements are heavily dependent on shared wireless communication lines. This dependency exposes data transmission pathways to sudden physical link deterioration, random electronic hardware gain fluctuations, or deceptive cyber-attacks. If these transient vulnerabilities are left unchecked by the state estimation system, they can trigger complete physical system failure before asymptotic

Corresponding Author: S. P. Sathiyapriya
Received: February 2026; Revised: June 2026; Accepted: August 2026.
https://doi.org/10.22111/ijfs.2026.54759.9692

stability rules can take effect. Therefore, designing a resilient filter that restricts states within a safe finite envelope under combined structural and malicious disturbances is an urgent practical requirement.

Nevertheless, the study of nonlinear systems remains challenging across many engineering domains since existing mathematical methods cannot fully assure global stability. To address this intricacy, the Takagi-Sugeno (T-S) fuzzy model approach is widely employed as a structured and effective control strategy [35]. This approach provides a systematic methodology to take full advantage of well-established linear control theory when exploring complex nonlinear plants [30]. Numerous significant findings regarding state estimation and control synthesis for T-S fuzzy systems have been documented using diverse approaches, such as standard filter design [24] and guaranteed-cost controller configurations [10]. The development of robust analytical methods for fuzzy systems has evolved from classical stability analysis techniques to intelligent control frameworks for complex networked environments. Robust analysis of fuzzy systems has progressed from classical stability methods to advanced control frameworks for constrained networked environments. Building on these developments, this paper addresses resilient extended passive filtering for switched systems under cyber-attacks. More broadly, fundamental analytical approaches have been extensively explored for analyzing and solving complex fuzzy mathematical models [15, 16, 21]. These foundational frameworks offer a versatile approach for handling complex, non-linear dynamics under uncertainty.

Compared to conventional strategies, a resilient filter under a switched Takagi-Sugeno (T-S) fuzzy framework offers distinct analytical and practical advantages. Recent research addresses severe network constraints, yielding non-fragile control for input-saturated systems with global prescribed performance via error-triggered mechanisms [33]. For a comprehensive survey of contemporary data-driven learning paradigms and adaptive structural modifications, see [2]. Furthermore, the work in [20] explores the design of finite-time mixed H_∞ and passivity filters for a specific group of uncertain nonlinear discrete-time Markovian jump systems characterized by a nonhomogeneous jump process. In [6], H_∞ and $L_2 - L_\infty$ filtering for discrete-time nonlinear switched systems with quantized measurements is addressed. An event-triggered fuzzy control design for inverted pendulum systems with time-varying delays was investigated in [25]. To establish a uniform framework, network-induced delays and adaptive backstepping data loss were addressed in parallel for nonlinear networked control systems in [31].

Additionally, the issue of reliable fuzzy filtering was studied in [14] for sensor networks by employing an interval type-2 fuzzy model-based control scheme. For stochastic nonlinear systems, an interval type-2 fuzzy approach featuring distributed soft fault detection over wireless sensor networks was presented in [7]. By utilizing a similar interval type-2 fuzzy configuration, a fault-tolerant sliding mode control strategy was reported in [37] for nonlinear systems experiencing parameter perturbations and distributed delays. Hence, it is highly essential to synthesize the coupling of switched systems and fuzzy models, commonly referred to as switched fuzzy systems. Increasing scientific attention has been focused on the resilient control of switched fuzzy networks due to their broad applications in single-link robot arm systems [3], tunnel diode circuits [11], and mass-spring damper mechanical assemblies [17]. For instance, a set of sufficient conditions was proposed for the fuzzy filter design of discrete-time nonlinear systems in [8], where three distinct filter designs were constructed to deal with low, middle, and high noise frequency domains, respectively [5].

Over the past couple of decades, state estimation has been a dynamically researched area due to its theoretical and practical significance in control layouts, communication networks, and signal processing. State estimation problems involve system states that cannot be directly measured. This limitation requires the design of an estimator based on available measured outputs. Various methodologies have been developed for this purpose, including H_∞ filtering [34], $L_2 - L_\infty$ filtering [38], dissipative filtering [18], and mixed H_∞ and passivity (extended passivity) filtering frameworks [4]. In [3], a robust stability framework was developed for discrete-time randomly switched fuzzy systems utilizing known sojourn probabilities, whereas the authors in [3] successfully demonstrated practical sampled-data control schemes tailored exclusively to F-18 aircraft switching dynamics. Similarly, the structural bounds of non-fragile control under actuator faults were evaluated in [11], which complements the foundational geometric layout of switched linear systems thoroughly detailed in [26]. Driven by its ability to enhance operational reliability, extended passive filtering has gained significant attention, as demonstrated by its application to discrete-time singular Markov jump systems with time-varying delays [32]. However, because physical implementations are prone to numerical round-off errors and hardware drifts [19], developing non-fragile filter structures that resist gain variations is essential [22], including under stochastic variations and channel fading [36]. Concurrently, there is growing interest in finite-time stability to bound trajectories over a fixed horizon, alongside Lyapunov and LMI techniques for event-triggered fuzzy systems [23, 25, 29]. In recent years, advanced filtering strategies, passivity conditions, and resilient state estimation for non-linear fuzzy networks have been extensively investigated [1, 27]. Resilient filtering ensures these non-linear systems maintain desired performance despite network disruptions. Despite these advancements, no published work has addressed finite-time resilient filtering with extended passivity for switched fuzzy systems subject to randomly occurring gain variations and varying sensor-actuator fault rates, inspiring this research.

In light of the factors outlined above, this study addresses the problem of resilient finite-horizon extended passive

filter design for a class of discrete-time switched fuzzy systems. These systems exhibit stochastic gain fluctuations and probabilistic faults in sensing or actuation components.
The primary contributions of this work are summarized as follows:

(i) A finite-time extended passive filtering framework with resilience against implementation uncertainties is proposed for switched fuzzy systems subject to probabilistic sensor/actuator failures with varying fault probabilities and randomly occurring gain deviations.

(ii) Novel sufficient criteria expressed in terms of linear matrix inequalities (LMIs) are derived for the construction of the extended passive filter, utilizing Lyapunov-based stability analysis in conjunction with finite-time theory.

(iii) The developed approach is versatile enough to handle additional complexities, including stochastic gain perturbations and probabilistic sensor/actuator malfunctions.

(iv) The obtained theoretical results are verified by numerical examples such as continuous-time single-link robot arm model and a tunnel diode circuit systems.

The remainder of this article is structured as follows: Section II provides the formal system descriptions, Takagi-Sugeno fuzzy rules, sensor fault models, and key mathematical definitions. Section III presents our main theoretical contributions, establishing linear matrix inequality conditions for robust finite-time stability and resilient filter synthesis. Section IV demonstrates the practical application of our findings using three comprehensive numerical simulation examples. Finally, Section V concludes the paper with a summary of key takeaways and suggestions for future research.

Notations: In this paper, the symbols "T" and "(-1)" as superscripts indicate matrix transposition and matrix inverse, respectively. $\mathbb{R}^n$ refers to the n-dimensional Euclidean space, while $\mathbb{R}^{n\times n}$ denotes the collection of all $n \times n$ real matrices. The notation $P > 0$ and $P < 0$ signifies that P is positive definite and negative definite, respectively. The space $L_2[0, \infty)$ denotes the set of n-dimensional square integrable functions over the interval $[0, \infty)$. The symbols I and 0 represent the identity matrix and zero matrix, respectively, with compatible dimensions. Within symmetric block matrices or lengthy matrix expressions, an asterisk $(*)$ is used to indicate a term derived from symmetry. The notation diag-represents a block-diagonal matrix.

2 System description and preliminaries

Switching may arise due to unexpected and sudden changes in system dynamics or structures, such as a rapid system structure transformation caused by component or subsystem failures. Moreover, intentional switching can be implemented to effectively control complex nonlinear systems described by either differential or difference switching systems. These switched systems typically involve sets of subsystems and switching signals that facilitate transitions between these subsystems. Here, we investigate the switched system in the discrete-time domain together with the jth fuzzy subsystem, which are presented in the subsequent formulation:

Model rule R_i^j : IF $\theta_{i1}(k)$ is F_{i1}^j and $\theta_{i2}(k)$ is F_{i2}^j and $\ldots$ and $\theta_{ip_i}(k)$ is $F_{ip_i}^j$, THEN

$$\begin{array}{rcl} x(k+1) &=& (A_{ij} + \Delta A_{ij}(k))x(k) + B_{ij}v(k), \\ y(k) &=& C_{ij}x(k) + D_{ij}v(k), \\ z(k) &=& H_{ij}x(k), \end{array} \tag{1}$$

where $x(k) \in \mathbb{R}^n$, $y(k) \in \mathbb{R}^m$ and $z(k) \in \mathbb{R}^q$ denotes the state, measurement and output signal; $v(k) \in \mathbb{R}^p$ represents the disturbance signal associated with $l_2[0, \infty)$; $\sigma(k) : [0, \infty) \to \mathcal{S} = \{1, 2, \ldots, \mathcal{N}\}$ is the switching signal, where $\mathcal{N}$ is the count of switching zones; $F_{i1}^j, F_{i2}^j, \cdots, F_{ip_i}^j$ indicates the fuzzy sets; $i \in \mathcal{S}$, $j \in L = \{1, 2, \ldots, r_i\}$ and r_i denotes how many inference rules are involved; $\theta_i = [\theta_{i1}(k), \theta_{i2}(k), \ldots, \theta_{ip_i}(k)]$ are the premise variables; A_{ij}, B_{ij}, C_{ij}, D_{ij}, H_{ij} and $\Delta A_{ij}(k)$ are the dimensioned matrices and uncertainty term of the jth model in the ith switching region of the systems, respectively. The condition stipulated for the external disturbance is $v(k)$:

$$\sum_{k=0}^{\infty} v^T(k)v(k) \leq \mathcal{V}, \tag{2}$$

where $\mathcal{V} \geq 0$ denotes the maximum admissible energy limit of the exogenous noise sequences within the $l_2[0,\infty)$ space. Further, to establish the necessary outcome, we enforce the following condition.

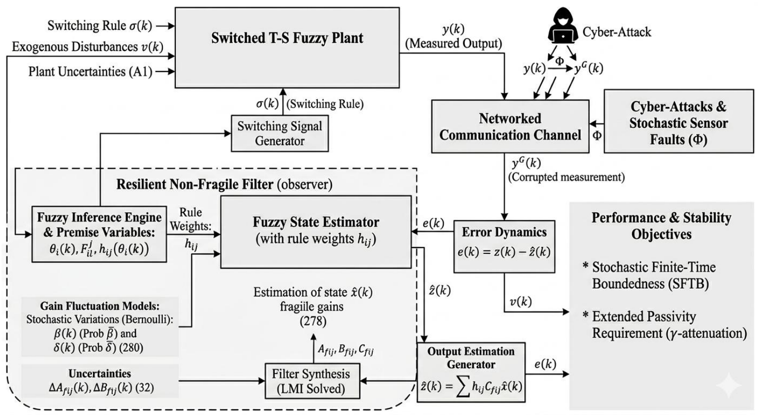

Figure 1: Block diagram of the proposed resilient switched fuzzy filtering architecture

(A1) Consider the indeterminate component associated with the jth local model within the ith switching region of the system satisfies $\Delta A_{ij}(k) = M_{ij} F_i(k) N_{aij}$, where the matrices M_{ij} and N_{aij} are prescribed matrices with explicitly known elements and suitable dimensions, whereas $F_i(k)$ represents a matrix of unknown values. This matrix consists of Lebesgue measurable elements that satisfy the condition $F_i^T(k) F_i(k) \leq I$ for all k. For ease of representation, we adopt $\bar{A}_{ij} = A_{ij} + \Delta A_{ij}(k)$. Applying the fuzzy inference rules yields the output of the discrete-time switched fuzzy system described as

$$\left.\begin{aligned} x(k+1) &= \sum_{j=1}^{r_i} h_{ij}(\theta(k))\big[\bar{A}_{ij}x(k) + B_{ij}v(k)\big], \\ y(k) &= \sum_{j=1}^{r_i} h_{ij}(\theta(k))\big[C_{ij}x(k) + D_{ij}v(k)\big], \\ z(k) &= \sum_{j=1}^{r_i} h_{ij}(\theta(k)) H_{ij}x(k), \end{aligned}\right\} \tag{3}$$

with $h_{ij}(\theta_i(k)) = \frac{\varphi_{ij}(\theta_i(k))}{\sum_{j=1}^{r_i} \varphi_{ij}(\theta_i(k))}$ and $\varphi_{ij}(\theta_i(k)) = \prod_{l=1}^{p_i} F_{il}^j(\theta_{il}(k))$. Hence, $F_{il}^i(\theta_{il}(k))$ is the function corresponds to a grade-based membership representation of $\theta_{il}(k)$ in F_{il}^i. It is assumed that $\varphi_{ij}(\theta_i(k)) \geq 0$ and $h_{ij}(\theta_i(k))$ satisfies $h_{ij}(\theta_i(k)) \geq 0$, $\sum_{j=1}^{r_i} h_{ij}(\theta_i(k)) = 1$ for all k, where $i \in \mathcal{S}$, $j \in L$.

In this paper, the sensor fault matrix $y^G(k)$ is adopted in the following form [13, 28]:

$$y^G(k) = \Phi y(k) = \sum_{l=1}^{m} \delta_l^2 \mathcal{C}_l y(k), \tag{4}$$

where Φ is the sensor fault matrix and it is partitioned into m terms, represented as $\Phi = \mathrm{diag}\{\zeta_1, \zeta_2, \ldots, \zeta_m\}$, where ζ_l are m independent random variables and, $\mathcal{C}_l = \mathrm{diag}\{0, \ldots, 0_{(l-1,l-1)}, 1_{(l,l)}, 0, \ldots, 0_{(m,m)}\}$. It is considered that ζ_l follows a probability density function $p_l(\zeta_l)$ defined over the interval $[0,1]$ with its mean value denoted by μ_l and corresponding variance δ_l^2 specified accordingly.For $P > 0$, by defining $\bar{\Phi} = \mathcal{E}\{\Phi\}$ and from (4), we have

$$\left\{\begin{aligned} &\mathcal{E}\{\Phi - \bar{\Phi}\} = 0, \\ &\mathcal{E}\{[\Phi - \bar{\Phi}]^T P [\Phi - \bar{\Phi}]\} = \sum_{l=1}^{m} \delta_l^2 \mathcal{C}_l^T P \mathcal{C}_l. \end{aligned}\right. \tag{5}$$

Here, the matrix notation $\bar{\Phi}$ denotes the deterministic mean value matrix of the stochastic sensor failure distribution. It is computed via the expectation operator such that $\bar{\Phi} = \mathcal{E}\{\Phi\} = \text{diag}\{\mu_1, \mu_2, \dots, \mu_m\}$. Now we introduce the design of a filter based on fuzzy-rule principles, tailored to the system under study that operates in a switching fuzzy framework.

$$\left.\begin{aligned} \hat{x}(k+1) &= \sum_{j=1}^{r_i} h_{ij}(\theta_i(k))(A_{fij}\hat{x}(k) + B_{fij}y^G(k)), \\ \hat{z}(k) &= \sum_{j=1}^{r_i} h_{ij}(\theta_i(k))C_{fij}\hat{x}(k). \end{aligned}\right\} \tag{6}$$

in which $\hat{x}(k)$ is used to indicate the state vector of the fuzzy filter, $\hat{z}(k)$ is the estimation of $z(k)$. Also A_{fij}, B_{fij} and C_{fij} represent the fuzzy filter parameters to be determined. Denoting $e(k) = z(k) - \hat{z}(k)$ and $\tilde{x}(k) = [x^T(k) \quad \hat{x}^T(k)]^T$, the extended formulation of (3), obtained by integrating the states of (6), is given as

$$\left.\begin{aligned} \tilde{x}(k+1) &= \sum_{j=1}^{r_i}\sum_{\eta=1}^{r_i} h_{ij}(\theta(k))h_{i\eta}(\theta(k))\big[\tilde{A}_{ij\eta}\tilde{x}(k) + \hat{B}_{i\eta}(\Phi-\bar{\Phi})\mathcal{H}_{ij}\tilde{x}(k) + \tilde{B}_{ij\eta}v(k) + \hat{B}_{i\eta}(\Phi-\bar{\Phi})D_{ij}v(k)\big], \\ e(k) &= \sum_{j=1}^{r_i}\sum_{\eta=1}^{r_i} h_{ij}(\theta(k))h_{i\eta}(\theta(k))\tilde{H}_{ij\eta}\tilde{x}(k), \end{aligned}\right\} \tag{7}$$

where $\tilde{A}_{ij\eta} = \begin{bmatrix} \bar{A}_{ij} & 0 \\ B_{fi\eta}\bar{\Phi}C_{ij} & A_{fi\eta} \end{bmatrix}$, $\tilde{B}_{ij\eta} = \begin{bmatrix} B_{ij} \\ B_{fi\eta}\bar{\Phi}D_{ij} \end{bmatrix}$, $\hat{B}_{i\eta} = \begin{bmatrix} 0 \\ B_{fi\eta} \end{bmatrix}$, $\tilde{H}_{ij\eta} = \begin{bmatrix} H_{ij} & -C_{fi\eta} \end{bmatrix}$, $\mathcal{H}_{ij} = \begin{bmatrix} C_{ij} & 0 \end{bmatrix}$.

The following definitions and lemmas will be used in the proof of the main results.

Definition 2.1. [20] *The augmented fuzzy system in* (7) *is robustly finite-time bounded with respect to* $(d_1, d_2, L, N, \mathcal{V})$, *where* $0 \le d_1 < d_2$, $L > 0$ *and* $\mathcal{V} \ge 0$, *if*

$$\mathcal{E}\{\tilde{x}(0)^T L\tilde{x}(0)\} \le d_1 \Rightarrow \mathcal{E}\{\tilde{x}(k)^T L\tilde{x}(k)\} < d_2, \forall\ k \in \{1, 2, \dots, N\},$$

applies to any non-zero $v(k)$ *that meets the condition in* (2).

Definition 2.2. [20] *The augmented fuzzy system in* (7) *is stochastically finite-time bounded with a prescribed extended passive performance index* γ *subject to* $(d_1, d_2, L, N, \alpha, \gamma)$, *where* L *is a positive definite matrix,* $\theta \in [0,\ 1]$, $0 \le d_1 < d_2$, *and positive scalar* γ, *if system* (7) *is stochastically finite-time bounded with respect to* (d_1, d_2, L, N, γ), *and under a zero initial condition, the output error* $e(k)$ *satisfies*

$$\mathcal{E}\Big\{\sum_{k=0}^{N}\big[\gamma^{-1}\theta e^T(k)e(k) - 2(1-\theta)e^T(k)v(k)\big]\Big\} \le \gamma\mathcal{E}\Big\{\sum_{k=0}^{N} v^T(k)v(k)\Big\},$$

for any non-zero $v(k)$ *satisfying* (2).

Lemma 2.3. [20] *Given constant matrices* X, Y *and* Z *where* $X = X^T$ *and* $0 < Y = Y^T$, *then* $X + Z^T Y^{-1} Z < 0$ *if and only if* $\begin{bmatrix} X & Z^T \\ * & -Y \end{bmatrix} < 0$ *or* $\begin{bmatrix} -Y & Z \\ * & X \end{bmatrix} < 0.$

Lemma 2.4. [20] *Given matrices* A, $Q = Q^T$ *and* $P > 0$, *then* $A^T PA - Q < 0$ *holds if and only if there exists a matrix* Y *such that* $\begin{bmatrix} -Q & A^T Y^T \\ * & P - Y - Y^T \end{bmatrix} < 0.$

Lemma 2.5. [20] *For any two matrices* X *and* Y *with appropriate dimensions, the inequality* $X^T Y + Y^T X \le \epsilon X^T X + \epsilon^{-1} Y^T Y$ *holds, where* $\epsilon > 0$.

Lemma 2.6. [3] *If the conditions* $\Upsilon_{ii} < 0, \quad 1 \le i \le r$ *and* $\frac{1}{r-1}\Upsilon_{ii} + \frac{1}{2}(\Upsilon_{ij} + \Upsilon_{ji}) < 0, \quad 1 \le i \ne j \le r$, *hold, then the inequality* $\sum_{i=1}^{r}\sum_{j=1}^{r}\omega_i\omega_j\Upsilon_{ij} < 0$ *holds, where* $\omega_i, \ \ 1 \le i \le r$ *satisfy* $0 \le \omega_i \le 1$ *and* $\sum_{i=1}^{r}\omega_i = 1$.

Definition 2.7. *It is to be noted that* [30] *for any* $k \ge k_0$ *and switching signal* $\sigma(l)$, $k_0 \le l < k$, *let* $N_\sigma(k_0, k)$ *denote the number of switchings of* $\sigma(k)$, *if* $N_\sigma(k_0, k) \le N_0 + \frac{k-k_0}{\tau_a}$ *holds, for* $N_0 \ge 0$ *and* $\tau_a > 0$, *then* τ_a *is called the average dwell time and* N_0 *is the chatter bound.*

3 Main results

This section is devoted to formulating a set of sufficient conditions that guarantee the finite-time boundedness of switched fuzzy systems through the application of a resilient extended passive filter described in (6). To this end, our principal contributions are presented in four theorems. Theorem 3.1 provides a sufficient criterion for achieving finite-time boundedness of the augmented fuzzy system given in (7), which serves as the foundation for the subsequent results. Building on Theorem 3.1, Theorem 3.2 incorporates an extended passive performance measure. Furthermore, Theorems 3.3 and 3.4 focus on the development of robust extended passive filters and resilient extended passive filters for the considered system, respectively. It is important to emphasize that all these results are obtained through the treatment of LMI-based conditions.

3.1 Finite-time boundedness analysis

In this section, we first derive the necessary condition in terms of LMIs to address the finite-time filtering problem. We then present sufficient criteria that ensure the finite-time filtering performance of the augmented fuzzy system. These results form the groundwork for the subsequent development of advanced filter designs.

Theorem 3.1. *For given scalars $\alpha \geq 1$, $\mu > 1$, the augmented fuzzy system in* (7) *with $\Delta A_{ij}(k) = 0$ is finite-time bounded with respect to $(d_1, d_2, L, N, \mathcal{V})$, if there exist symmetric positive definite matrices P_i, W and positive scalars λ_1, λ_2, such that the following matrix inequalities hold:*

$$\Theta_{ijj} < 0, \; 1 \leq j \leq r_i, \tag{8}$$

$$\frac{1}{r-1}\Theta_{ijj} + \frac{1}{2}(\Theta_{ij\eta} + \Theta_{i\eta j}) < 0, \; 1 \leq j \neq \eta \leq r_i, \tag{9}$$

$$P_{ij} \leq \mu P_{i' j'}, \; i^{'} \in \mathcal{S}, \; j^{'} \in L \tag{10}$$

$$\begin{bmatrix} -\bar{P}_i^{-1} & \lambda_1 \bar{P}_i^{-1} L \\ * & -\lambda_1 L \end{bmatrix} < 0, \quad \begin{bmatrix} -\lambda_2 L & I \\ * & \bar{P}_i^{-1} \end{bmatrix} < 0, \tag{11}$$

$$d_1 \lambda_2 + \lambda_3 \mathcal{V} < d_2 \alpha^{-N} \lambda_1, \tag{12}$$

with the switching signal $\sigma(k)$ meeting the average dwell-time condition $\tau > \frac{N ln\mu}{ln\kappa_1 - ln\kappa_2} = \tau^*$, where

$$\Theta_{ij\eta} = \begin{bmatrix} \Theta_{1i} & \Theta_{2ij\eta} & \Theta_{3ij\eta} & \Theta_{5ij\eta} \\ * & -P_i & 0 & 0 \\ * & * & \Theta_{4i} & 0 \\ * & * & * & \Theta_{6i} \end{bmatrix}, \quad \Theta_{1i} = \begin{bmatrix} -\alpha P_i & 0 \\ * & -\alpha W \end{bmatrix}, \quad \Theta_{2ij\eta} = \begin{bmatrix} \tilde{A}_{ij\eta}^T P_i \\ \tilde{B}_{ij\eta}^T P_i \end{bmatrix},$$

$$\Theta_{3ij\eta} = \begin{bmatrix} \delta_1 \mathcal{H}_{ij}^T \mathcal{C}_1^T \hat{B}_{i\eta}^T P_i & \dots & \delta_m \mathcal{H}_{ij}^T \mathcal{C}_m^T \hat{B}_{i\eta}^T P_i \\ 0 & \dots & 0 \end{bmatrix}, \quad \Theta_{4i} = diag\{\underbrace{-P_i \cdots - P_i}_{m}\},$$

$$\Theta_{5ij\eta} = \begin{bmatrix} 0 & \dots & 0 \\ \delta_1 D_{ij}^T \mathcal{C}_1^T \hat{B}_{i\eta}^T P_i & \dots & \delta_m D_{ij}^T \mathcal{C}_m^T \hat{B}_{i\eta}^T P_i \end{bmatrix}, \quad \Theta_{6i} = diag\{\underbrace{-P_i \cdots - P_i}_{m}\},$$

$$\kappa_1 = (\mu - 1) d_2 \lambda_1 \alpha^{-N} + \mathcal{V}\lambda_3, \quad \kappa_2 = d_1 \lambda_2 (\mu - 1) + \mathcal{V}\lambda_3, \quad \lambda_1 = \min_{i \in \mathcal{S}} \{\lambda_{\min}(\bar{P}_i)\},$$

$$\lambda_2 = \max_{i \in \mathcal{S}} \{\lambda_{\max}(\bar{P}_i)\}, \quad \lambda_3 = \max_{i \in \mathcal{S}} \{\lambda_{\max}(W)\}, \quad \bar{P}_i = L^{-1/2} P_i L^{-1/2},$$

and for every permissible $v(k)$ that satisfies condition (2).

Proof. We consider a quadratic Lyapunov function tailored to the switching modes for system (7):

$$V_i(k) = \tilde{x}^T(k) P_i(k) \tilde{x}(k). \tag{13}$$

Evaluating the forward increment of the chosen candidate Lyapunov function along the system trajectories in (7) and taking its expected value, we arrive at

$$\begin{aligned}
\mathcal{E}\Big\{\Delta V_i(k)-(\alpha-1)V_i(k)\Big\} =&\mathcal{E}\Big\{V_i(k+1)-\alpha V_i(k)\Big\}\\
=&\mathcal{E}\Big\{\tilde{x}^T(k+1)P_i(k+1)\tilde{x}(k+1)-\alpha\tilde{x}^T(k)P_i(k)\tilde{x}(k)\Big\}\\
=&\mathcal{E}\Big\{\sum_{j=1}^{r_i}\sum_{\eta=1}^{r_i}\sum_{j'=1}^{r_i}\sum_{\eta'=1}^{r_i}h_{ij}(\theta(k))h_{i\eta}(\theta(k))h_{ij'}(\theta(k))h_{i\eta'}(\theta(k))\\
&\times\big[\tilde{A}_{ij\eta}\tilde{x}(k)+\hat{B}_{i\eta}(\Phi-\bar{\Phi})\mathcal{H}_{ij}\tilde{x}(k)+\tilde{B}_{ij\eta}v(k)+\hat{B}_{i\eta}(\Phi-\bar{\Phi})D_{ij}v(k)\big]^T\\
&\times P_i(k+1)\big[\tilde{A}_{ij\eta}\tilde{x}(k)+\hat{B}_{i\eta}(\Phi-\bar{\Phi})\mathcal{H}_{ij}\tilde{x}(k)+\tilde{B}_{ij\eta}v(k)+\hat{B}_{i\eta}(\Phi-\bar{\Phi})D_{ij}v(k)\big]\\
&-\alpha\tilde{x}^T(k)P_i(k)\tilde{x}(k)\Big\}\\
\le&\sum_{j=1}^{r_i}\sum_{\eta=1}^{r_i}h_{ij}(\theta(k))h_{i\eta}(\theta(k))\\
&\times\Big\{\big[\tilde{A}_{ij\eta}\tilde{x}(k)+\tilde{B}_{ij\eta}v(k)\big]^TP_i(k+1)\big[\tilde{A}_{ij\eta}\tilde{x}(k)+\tilde{B}_{ij\eta}v(k)\big]\\
&-\alpha\tilde{x}^T(k)P_i(k)\tilde{x}(k)+\mathcal{E}\big\{\tilde{x}^T(k)\mathcal{H}_{ij}^T(\Phi-\bar{\Phi})^T\hat{B}_{i\eta}^TP_i(k+1)\hat{B}_{i\eta}(\Phi-\bar{\Phi})\mathcal{H}_{ij}\tilde{x}(k)\big\}\\
&+\mathcal{E}\big\{v^T(k)D_{ij}^T(\Phi-\bar{\Phi})^T\hat{B}_{i\eta}^TP_i(k+1)\hat{B}_{i\eta}(\Phi-\bar{\Phi})D_{ij}v(k)\big\}\Big\}. \qquad (14)
\end{aligned}$$

Based on the results of (5) and (14), we obtain that

$$\mathcal{E}\big\{\tilde{x}^T(k)\mathcal{H}_{ij}^T(\Phi-\bar{\Phi})^T\hat{B}_{i\eta}^TP_i(k+1)\hat{B}_{i\eta}(\Phi-\bar{\Phi})\mathcal{H}_{ij}\tilde{x}(k)\big\}=\tilde{x}^T(k)\sum_{l=1}^{m}\delta_l^2\mathcal{H}_{ij}^T\mathcal{C}_l^T\hat{B}_{i\eta}^TP_i(k+1)\hat{B}_{i\eta}\mathcal{C}_l\mathcal{H}_{ij}\tilde{x}(k), \qquad (15)$$

and

$$\mathcal{E}\big\{v^T(k)D_{ij}^T(\Phi-\bar{\Phi})^T\hat{B}_{i\eta}^TP_i(k+1)\hat{B}_{i\eta}(\Phi-\bar{\Phi})D_{ij}v(k)\big\}=v^T(k)\sum_{l=1}^{m}\delta_l^2D_{ij}^T\mathcal{C}_l^T\hat{B}_{i\eta}^TP_i(k+1)\hat{B}_{i\eta}\mathcal{C}_lD_{ij}v(k). \qquad (16)$$

Now, combining (14)-(16), we arrive at

$$\mathcal{E}\big[\Delta V_i(k)-(\alpha-1)V_i(k)-\alpha v^T(k)Wv(k)\big]\le\Big[\xi^T(k)\Big(\Theta_{1i}+\Theta_{2ij\eta}^TP_i^{-1}\Theta_{2ij\eta}+\Theta_{3ij\eta}^TP_i^{-1}\Theta_{3ij\eta}+\Theta_{4ij\eta}^TP_i^{-1}\Theta_{4ij\eta}\Big)\xi(k)\Big], \qquad (17)$$

where $\xi^T(k)=\big[\tilde{x}^T(k)\quad v^T(k)\big]^T$ and $P_i=P_i(k+1)$. Employing the Schur complement in (17) leads to $\Theta_{ij\eta}$, as outlined in the theorem. Hence, if the LMIs (8) and (9) hold, it is easy to obtain that

$$V(k+1)\le\alpha\tilde{x}^T(k)P_i\tilde{x}(k)+\alpha v^T(k)Wv(k). \qquad (18)$$

The preceding inequality implies that $V_{\sigma(k)}(k)\le\alpha^{k-k_l}V_{\sigma(k_l)}(k_l)+\sum\limits_{s=k_l}^{k-1}\alpha^{k-s}v^T(s)Wv(s)$.

Note that $V_{\sigma(k_l)}(k_l)\le\mu V_{\sigma(k_{l-1})}(k_l)$ and $V_{\sigma(k_{l-1})}(k_l)\le\mu\alpha^{k_l-k_{l-1}}V_{\sigma(k_{l-1})}(k_{l-1})+\sum\limits_{s=k_{l-1}}^{k_l-1}\alpha^{k_l-s}v^T(s)Wv(s)$. It yields that $V_{\sigma(k_l)}(k_l)\le\mu\alpha^{k_l-k_{l-1}}V_{\sigma(k_{l-1})}(k_{l-1})+\mu\sum\limits_{s=k_{l-1}}^{k_l-1}\alpha^{k_l-s}v^T(s)Wv(s)$. By using the above relations, we can get

$$\begin{aligned}
V_{\sigma(k)}(k)&\le\mu\alpha^{k-k_{l-1}}V_{\sigma(k_{l-1})}(k_{l-1})+\mu\sum_{s=k_{l-1}}^{k_l-1}\alpha^{k_l-s}v^T(s)Wv(s)\\
&\le\mu\alpha^{k-k_{l-1}}V_{\sigma(k_{l-1})}(k_{l-1})+\mu\alpha^k\mathcal{V}\lambda_{\max}(W)\\
&\le\mu^2\alpha^{k-k_{l-2}}V_{\sigma_{k_{l-2}}}(k_{l-2})+\mu\alpha^k\mathcal{V}\lambda_{\max}(W)+\alpha^k\mathcal{V}\lambda_{\max}(W)
\end{aligned}$$

$$
\begin{aligned}
&\leq \ \dots \\
&\leq \ \alpha^{k-k_0}\mu^{\frac{k-k_0}{\tau_a}} V_{\sigma(k_0)}(k_0) + \mathcal{V}\lambda_{\max}(W)\alpha^k \sum_{s=1}^{(k-k_0)/\tau_a} \mu^{\frac{k-k_0}{\tau_a - 1} - s} \\
&\leq \ \alpha^{k-k_0}\mu^{\frac{k-k_0}{\tau_a}} \tilde{x}^T(k_0)_i P\tilde{x}(k_0) + \alpha^k \mathcal{V}\lambda_{\max}(W)\frac{\mu^{k/\tau_a} - 1}{\mu - 1} \\
&\leq \ \alpha^{k-k_0}\mu^{\frac{k-k_0}{\tau_a}} \sup\{\lambda_{\max}(\bar{P}_i)\tilde{x}^T(k_0)L\tilde{x}(k_0) + \alpha^k\mathcal{V}\lambda_{\max}(W)\frac{\mu^{k/\tau_a} - 1}{\mu - 1}\} \\
&\leq \ \alpha^N\big(\mu^{\frac{N}{\tau_a}} d_1\big)\bigg(\mu^{\frac{N}{\tau_a}} \sup_i \lambda_{\max}(\bar{P}_i) + \frac{\mu^{k/\tau_a} - 1}{\mu - 1}\bigg).
\end{aligned}
$$

Also, we observe that $V_i(k) \geq \tilde{x}^T(k)P_i\tilde{x}(k) \geq \lambda_1\tilde{x}^T(k)L\tilde{x}(k)$. Then, we can obtain

$$
\tilde{x}^T(k)L\tilde{x}(k) \leq \frac{\alpha^N}{\lambda_1}\bigg\{\frac{\kappa_1}{\kappa_2}d_1\lambda_2 + \mathcal{V}\lambda_3 + \frac{\frac{\kappa_1}{\kappa_2} - 1}{\mu - 1}\mu\alpha^N\mathcal{V}\lambda_3\bigg\}.
$$

From (11), we have $\lambda_1 L < P < \lambda_2 L \quad \Rightarrow \quad \lambda_1 I < \bar{P}_i < \lambda_2 I$. Since $\sup_i\{\lambda_{\max}(\bar{P}_i)\} \leq \lambda_2$, $\inf_i\{\lambda_{\min}(\bar{P}_i)\} \geq \lambda_1$ and by condition (12), it follows that $\tilde{x}^T(k)L\tilde{x}(k) < \bigg\{\mu^{\frac{N}{\tau_a}} d_1\lambda_2 + \frac{\mu^{k/\tau_a} - 1}{\mu - 1}\mathcal{V}\lambda_3\bigg\} = d_2$. Therefore, it is concluded that the system (7) exhibits finite-time boundedness concerning $(d_1, d_2, L, N, \mathcal{V})$. The proof for this theorem is now concluded. □

3.2 Finite-time extended passivity performance analysis

We present sufficient criteria for the augmented fuzzy system in (7) to remain stochastically stable within a finite horizon under a broadened passivity measure, as shown in Theorem 3.1.

Theorem 3.2. *If certain scalars hold specifically $\alpha \geq 1$ and $\mu > 1$, and if the augmented fuzzy system described in* (7) *with $\Delta A_{ij}(k) = 0$ satisfies the specified matrix inequalities alongside* (10)*, and assuming the availability of a symmetric positive definite matrix P_i along with positive scalars $0 \leq d_1 < d_2$, λ_1, λ_2, then it exhibits finite-time bounded behavior concerning the extended passive performance criteria* $(d_1, d_2, L, N, \mathcal{V}, \gamma)$.

$$
\hat{\Theta}_{ijj} \quad < \quad 0, \ 1 \leq j \leq r_i, \tag{19}
$$

$$
\frac{1}{r-1}\hat{\Theta}_{ijj} + \frac{1}{2}(\hat{\Theta}_{ij\eta} + \hat{\Theta}_{i\eta j}) \quad < \quad 0, \ 1 \leq j \neq \eta \leq r_i, \tag{20}
$$

$$
d_1\lambda_2 + \gamma\mathcal{V} < d_2\alpha^{-N}\lambda_1, \tag{21}
$$

with the switching signal $\sigma(k)$ governed by an average dwell-time rule $\tau > \frac{Nln\mu}{ln\kappa_1 - ln\kappa_2} = \tau^*$, where

$$
\hat{\Theta}_{ij\eta} = \begin{bmatrix} \bar{\Theta}_{ij\eta} & \bar{\Theta}_{7ij\eta}^T \\ * & -\gamma I \end{bmatrix}, \quad \bar{\Theta}_{ij\eta} = \begin{bmatrix} \bar{\Theta}_{1ij\eta} & \bar{\Theta}_{2ij\eta} & \bar{\Theta}_{3ij\eta} & \bar{\Theta}_{5ij\eta} \\ * & -P_i & 0 & 0 \\ * & * & \bar{\Theta}_{4i} & 0 \\ * & * & * & \bar{\Theta}_{6i} \end{bmatrix}, \quad \bar{\Theta}_{1ij\eta} = \begin{bmatrix} -\alpha P_i & -(1-\theta)\tilde{H}_{ij\eta}^T \\ * & -\gamma I \end{bmatrix},
$$

$$
\bar{\Theta}_{2ij\eta} = \Theta_{2ij\eta}, \quad \bar{\Theta}_{3ij\eta} = \Theta_{3ij\eta}, \quad \bar{\Theta}_{4i} = \Theta_{4i}, \quad \bar{\Theta}_{5ij\eta} = \Theta_{5ij\eta}, \quad \bar{\Theta}_{6i} = \Theta_{6i}, \quad \bar{\Theta}_{7ij\eta} = \begin{bmatrix} \sqrt{\theta}\hat{H}_{ij\eta} & 0 & 0 & 0 \end{bmatrix},
$$

$$
\hat{H}_{ij\eta} = \begin{bmatrix} \tilde{H}_{ij\eta} & 0 \end{bmatrix}, \ \kappa_1 = (\mu - 1)d_2\lambda_1\alpha^{-N} + \mathcal{V}\gamma, \quad \kappa_2 = d_1\lambda_2(\mu - 1) + \mathcal{V}\gamma, \lambda_1 = \min_{i\in M}\{\lambda_{\min}(\bar{P}_i)\},
$$

$\lambda_2 = \max_{i\in M}\{\lambda_{\max}(\bar{P}_i)\}$ *and the other parameters are defined as same in Theorem 3.1.*

Proof. We examine the extended passive behavior of system (7), with the definition of $\mathcal{J}(k)$ as: $\mathcal{J}(k) = \gamma^{-1}\theta e^T(k)e(k) - 2(1-\theta)e^T(k)v(k) - \gamma v^T(k)v(k)$. A procedure parallel to that in Theorem 3.1 is employed, where $W = \gamma I$ is substituted in $\mathcal{J}(k)$, and the reasoning mirrors the development of (14).

$$
\mathcal{E}\{V_i(k+1) - \alpha V_i(k) + \mathcal{J}(k)\} \leq \Big[\xi^T(k)\Big(\bar{\Theta}_{ij\eta} + \bar{\Theta}_{7ij\eta}^T\bar{\Theta}_{7ij\eta}\Big)\xi(k)\Big]. \tag{22}
$$

By using the Schur complement, (19) and (20) guarantee that

$$V_i(k+1) - \alpha V_i(k) + \mathcal{J}(k) < 0. \tag{23}$$

Based on the above inequality, a recursive relation takes the form

$$V_{\sigma(k)}(k) < \alpha^{k-k_0} V(\tilde{x}(k_0), \sigma(k)) - \sum_{l=k_0}^{k-1} \alpha^{k-l-1} \mathcal{J}(l). \tag{24}$$

It follows from (23) and (24) that

$$\begin{aligned}
V_{\sigma(k)}(k) &\leq \alpha^{k-k_s} V(\tilde{x}(k_s), \sigma(k)) - \sum_{l=k_s}^{k-1} \alpha^{k-l-1} \mathcal{J}(l) \\
&\leq \alpha^{k-k_s} \mu V(\tilde{x}(k_s), \sigma(k_{s-1})) - \sum_{l=k_s}^{k-1} \alpha^{k-l-1} \mathcal{J}(l) \\
&\leq \alpha^{k-k_s} \mu \big[\alpha^{k_s-k_{s-1}} V(\tilde{x}(k_{s-1}), \sigma(k_{s-1})) + \sum_{l=k_{s-1}}^{k-1} \alpha^{k_s-l-1} \mathcal{J}(l)\big] - \sum_{l=k_s}^{k-1} \alpha^{k-l-1} \mathcal{J}(l) \\
&\leq \alpha^{k-k_{s-1}} \mu^2 \big[\alpha^{k_{s-1}-k_{s-2}} V(\tilde{x}(k_{s-2}), \sigma(k_{s-2})) - \sum_{l=k_{s-2}}^{k_{s-1}-1} \alpha^{k_{s-1}-l-1} \mathcal{J}(l)\big] \\
&- \alpha^{k-k_s} \mu \sum_{l=k_{s-1}}^{k_s-1} \alpha^{k_s-l-1} \mathcal{J}(l) - \sum_{l=k_s}^{k-1} \alpha^{k-l-1} \mathcal{J}(l) \\
&\leq \dots \\
&\leq \alpha^{k-k_0} \mu^{N(k_0,k)} V(\tilde{x}(k_0), \sigma(k_0)) - \alpha^{k-k_s} \mu^{N(k_0,k)} \sum_{l=k_0}^{k_s-1} \alpha^{k_s-l-1} \mathcal{J}(l) \\
&- \alpha^{k-k_2} \mu^{N(k_s,k)} \sum_{l=k_s}^{k_2-1} \alpha^{k_2-l-1} \mathcal{J}(l) - \dots - \sum_{l=k_0}^{k-1} \mu^{N(l,k)} \alpha^{k-l-1} \mathcal{J}(l).
\end{aligned}$$

Assuming a zero initial state and noting that $V(\tilde{x}(k)) \geq 0$ for every $k \in 1, 2, \dots, N$, it follows directly that

$$\mathcal{E}\Big\{\sum_{k=0}^{N} \big[\gamma^{-1}\theta e^T(k)e(k) - 2(1-\theta)e^T(k)v(k)\big]\Big\} \leq \gamma \mathcal{E}\Big\{\sum_{k=0}^{N} v^T(k)v(k)\Big\}. \tag{25}$$

Thus, utilizing (25), deriving the inequality outlined in Definition 2.2 becomes straightforward. Thus, it follows that system (7) exhibits stochastic stability within a finite duration while also satisfying a specified extended passivity criterion. This concludes the proof. □

3.3 Robust finite-time extended passive filter design

Building on Theorem 3.2, we present the design methodology for the extended passive filter over a specified finite-time interval for system (7).

Theorem 3.3. *Given scalars $\alpha \geq 1$, $\mu > 1$, and a matrix L, the augmented fuzzy system described in equation (7) demonstrates robust stochastic finite-time boundedness with a specified generalized passivity criterion, subject to the conditions $(0, d_2, L, N, \mathcal{V}, \gamma)$. These conditions hold under the existence of symmetric positive definite matrices P_{1i}, P_{3i}, as well as matrices P_{2i}, S_i, Z_i, Y_i, A_{Fij}, B_{Fij}, and C_{Fij}, along with a scalar $d_2 > 0$. These conditions are satisfied when the following LMIs are met in conjunction with equation (10):*

$$\Sigma_{ijj} < 0, \ 1 \leq j \leq r_i, \tag{26}$$

$$\frac{1}{r-1}\Sigma_{ijj} + \frac{1}{2}(\Sigma_{ij\eta} + \Sigma_{i\eta j}) < 0, \ 1 \leq j \neq \eta \leq r_i, \tag{27}$$

$$\bar{\lambda}_1\gamma\mathcal{V} < d_2\alpha^{-N}, \tag{28}$$

provided that the switching signal $\sigma(k)$ complies with an average dwell-time condition

$$\tau > \frac{Nln\mu}{ln\kappa_1 - ln\gamma - ln\mathcal{V}} = \tau^*, \tag{29}$$

where

$$\Sigma_{ij\eta} = \begin{bmatrix} \hat{\Sigma}_{ij\eta} & \epsilon_{1i}\bar{\Sigma}_{1ij}^T & \bar{\Sigma}_{2ij} \\ * & -\epsilon_{1i} & 0 \\ * & * & -\epsilon_{1i} \end{bmatrix}, \quad \hat{\Sigma}_{ij\eta} = \begin{bmatrix} \hat{\Sigma}_{1ij\eta} & \hat{\Sigma}_{2ij\eta} & \hat{\Sigma}_{4ij\eta} & \hat{\Sigma}_{6ij\eta} & \hat{\Sigma}_{7ij\eta}^T \\ * & \hat{\Sigma}_{3i} & 0 & 0 & 0 \\ * & * & \hat{\Sigma}_{5i} & 0 & 0 \\ * & * & * & \hat{\Sigma}_{5i} & 0 \\ * & * & * & * & -\gamma I \end{bmatrix},$$

$$\hat{\Sigma}_{1ij\eta} = \begin{bmatrix} -\alpha P_{1i} & -\alpha P_{2i} & -(1-\theta)H_{ij}^T \\ * & -\alpha P_{3i} & (1-\theta)C_{Fi\eta}^T \\ * & * & -\gamma I \end{bmatrix}, \quad \hat{\Sigma}_{2ij\eta} = \begin{bmatrix} A_{ij}^T S_i^T + C_{ij}^T\bar{\Phi}^T B_{Fi\eta}^T & A_{ij}^T Z_i^T + C_{ij}^T\bar{\Phi}^T B_{Fi\eta}^T \\ A_{Fi\eta}^T & A_{Fi\eta}^T \\ B_{ij}^T S_i^T + D_{ij}^T\bar{\Phi}^T B_{Fi\eta}^T & B_{ij}^T Z_i^T + D_{ij}^T\bar{\Phi}^T B_{Fi\eta}^T \end{bmatrix},$$

$$\hat{\Sigma}_{3i} = \begin{bmatrix} P_{1i} - S_i - S_i^T & P_{2i} - Y_i - Z_i^T \\ * & P_{3i} - Y_i - Y_i^T \end{bmatrix},$$

$$\hat{\Sigma}_{4ij\eta} = \begin{bmatrix} \delta_1 C_{ij}^T\mathcal{C}_1^T B_{Fi\eta}^T & \delta_1 C_{ij}^T\mathcal{C}_1^T B_{Fi\eta}^T & \cdots & \delta_m C_{ij}^T\mathcal{C}_m^T B_{Fi\eta}^T & \delta_m C_{ij}^T\mathcal{C}_m^T B_{Fi\eta}^T \\ 0 & 0 & \cdots & 0 & 0 \\ 0 & 0 & \cdots & 0 & 0 \end{bmatrix},$$

$$\hat{\Sigma}_{5i} = \begin{bmatrix} P_{1i} - S_i - S_i^T & P_{2i} - Y_i - Z_i^T & \cdots & 0 & 0 \\ * & P_{3i} - Y_i - Y_i^T & \cdots & 0 & 0 \\ * & * & \ddots & \cdots & \cdots \\ * & * & * & P_{1i} - S_i - S_i^T & P_{2i} - Y_i - Z_i^T \\ * & * & * & * & P_{3i} - Y_i - Y_i^T \end{bmatrix},$$

$$\hat{\Sigma}_{6ij\eta} = \begin{bmatrix} 0 & 0 & \cdots & 0 & 0 \\ 0 & 0 & \cdots & 0 & 0 \\ \delta_1 D_{ij}^T\mathcal{C}_1^T B_{Fi\eta}^T & \delta_1 D_{ij}^T\mathcal{C}_1^T B_{Fi\eta}^T & \cdots & \delta_m D_{ij}^T\mathcal{C}_m^T B_{Fi\eta}^T & \delta_m D_{ij}^T\mathcal{C}_m^T B_{Fi\eta}^T \end{bmatrix},$$

$$\hat{\Sigma}_{7ij\eta} = \begin{bmatrix} \sqrt{\theta}H_{ij} & -\sqrt{\theta}C_{Fi\eta} & 0 \end{bmatrix}, \quad \bar{\Sigma}_{1ij} = \begin{bmatrix} \Sigma_{8ij} & 0_{4n} \end{bmatrix}, \quad \bar{\Sigma}_{2ij}^T = \begin{bmatrix} 0 & \Sigma_{9ij} & 0_{3n} \end{bmatrix},$$

$$\Sigma_{8ij} = \begin{bmatrix} N_{aij} & 0 & 0 \end{bmatrix}, \ \Sigma_{9ij} = \begin{bmatrix} M_{ij}^T S_i^T & M_{ij}^T Z_i^T \end{bmatrix}, \ \kappa_1 = (\mu - 1)\frac{d_2}{\bar{\lambda}_1}\alpha^{-N} + \gamma\mathcal{V}.$$

The filter's gain matrices are accordingly expressed as: $A_{fij} = Y_i^{-1}A_{Fij}$, $B_{fij} = Y_i^{-1}B_{Fij}$, and $C_{fij} = C_{Fij}$.

Proof. Let U_i and P_i be defined as partition matrices in the following manner:

$$P_i = \begin{bmatrix} P_{1i} & P_{2i} \\ * & P_{3i} \end{bmatrix} \quad \text{and} \quad U_i = \begin{bmatrix} S_i & Y_i \\ Z_i & Y_i \end{bmatrix}.$$

Through the use of Lemma 2.4 on the inequalities (19) and (20), in combination with the partitioned matrices P_i and U_i, we derive

$$\begin{bmatrix} \Sigma_{1ij\eta} & \Sigma_{2ij\eta} & \Sigma_{3ij\eta} & \Sigma_{5ij\eta} & \Sigma_{7ij\eta}^T \\ * & P_i - U_i - U_i^T & 0 & 0 & 0 \\ * & * & \Sigma_{4i} & 0 & 0 \\ * & * & * & \Sigma_{6i} & 0 \\ * & * & * & * & -I \end{bmatrix} < 0, \tag{30}$$

where

$$\Sigma_{1ij\eta} = \begin{bmatrix} -\alpha P_i & \tilde{H}_{ij\eta}^T \mathcal{S} \\ * & -\mathcal{R} \end{bmatrix}, \quad \Sigma_{2ij\eta} = \begin{bmatrix} \tilde{A}_{ij\eta}^T U_i^T \\ \tilde{B}_{ij\eta}^T U_i^T \end{bmatrix}, \ \Sigma_{3ij\eta} = \begin{bmatrix} \delta_1 \mathcal{H}_{ij}^T \mathcal{C}_1^T \hat{B}_{i\eta}^T U_i^T & \dots & \delta_m \mathcal{H}_{ij}^T \mathcal{C}_m^T \hat{B}_{i\eta}^T U_i^T \\ 0 & \dots & 0 \end{bmatrix},$$

$$\Sigma_{4i} = \mathrm{diag}\{\underbrace{P_i - U_i - U_i^T \dots P_i - U_i - U_i^T}_{m}\}, \ \Sigma_{5ij\eta} = \begin{bmatrix} 0 & \dots & 0 \\ \delta_1 D_{ij}^T \mathcal{C}_1^T \hat{B}_{i\eta}^T U_i^T & \dots & \delta_m D_{ij}^T \mathcal{C}_m^T \hat{B}_{i\eta}^T U_i^T \end{bmatrix},$$

$$\Sigma_{6i} = \mathrm{diag}\{\underbrace{P_i - U_i - U_i^T \dots P_i - U_i - U_i^T}_{m}\}, \ \Sigma_{7ij\eta} = \begin{bmatrix} \sqrt{\mathcal{Q}} \tilde{H}_{ij\eta} & 0 \end{bmatrix}.$$

By letting $A_{Fij} = Y_i A_{fij}$, $B_{Fij} = Y_i B_{fij}$, $C_{Fij} = C_{fij}$ and by employing the parameter uncertainty specified in **A1**, the preceding matrix inequality is reformulated as:

$$\hat{\Sigma}_{ij\eta} + \bar{\Sigma}_{1ij}^T F_i^T(k) \bar{\Sigma}_{2ij}^T + \bar{\Sigma}_{2ij} F_i(k) \bar{\Sigma}_{1ij} < 0. \tag{31}$$

Moreover, applying Lemmas 2.4 and 2.5 to (31) yields the LMIs (26) and (27), thereby completing the proof of this theorem. This establishes the required result under the given conditions.

Filter parameter synthesis procedure to systematically construct the filter gains without relying on heuristic methods, the design parameters must be evaluated using the following sequence:

Step 1: Select the finite-time expansion scalar $\alpha \geq 1$, the ADT mode adjustment scalar $\mu > 1$, the performance weighting coefficient $\theta \in [0, 1]$, and the target attenuation index $\gamma > 0$ based on physical system constraints.

Step 2: Input your system matrices $(A_{ij}, B_{ij}, C_{ij}, D_{ij}, H_{ij})$ into the LMI solver to compute the symmetric positive definite matrices P_{1i}, P_{3i} and auxiliary matrices $S_i, Z_i, Y_i, A_{Fij}, B_{Fij}, C_{Fij}$ using conditions (26) - (27).

Step 3: Once numerical feasibility is confirmed, compute the actual non-fragile filter parameters directly using the exact algebraic conversions: $A_{fij} = Y_i^{-1} A_{Fij}, \quad B_{fij} = Y_i^{-1} B_{Fij}, \quad C_{fij} = C_{Fij}$.

□

3.4 Resilient finite-time extended passive filter design

In this subsection, we focus on deriving a resilient extended passive filter design for the augmented fuzzy system in (7). At this stage, the gains $\bar{A}fij$ and $\bar{B}fij$ are expressed as $\bar{A}fij = Afij + \beta(k)\Delta Afij(k)$ and $\bar{B}fij = Bfij + \delta(k)\Delta Bfij(k)$. The uncertain perturbations $\Delta Afij(k)$ and $\Delta Bfij(k)$ are specified below:

$$\Delta A_{fij}(k) = \mathcal{M}_{ij} \Delta_i(k) \mathcal{N}_{aij} \quad \text{and} \quad \Delta B_{fij}(k) = \mathcal{M}_{ij} \Delta_i(k) \mathcal{N}_{bij}, \tag{32}$$

where the matrices $\mathcal{M}ij$, $\mathcal{N}aij$, and $\mathcal{N}_{bij}$ are fixed and known, whereas $\Delta_i(k)$ denotes a matrix uncertainty constrained by $\Delta_i(k)^T \Delta_i(k) \leq I$. In addition, $\beta(k)$ and $\delta(k)$ are random sequences characterizing stochastic variations in the filter gain. Both $\beta(k)$ and $\delta(k)$ are modeled as Bernoulli white processes, each assuming values 0 or 1 with probabilities $Pr\beta(k) = 1 = \mathcal{E}\beta(k) = \bar{\beta}$ and $Pr\delta(k) = 1 = \mathcal{E}\delta(k) = \bar{\delta}$, where $\bar{\beta}, \bar{\delta} \in [0, 1]$. Correspondingly, $Pr\beta(k) = 0 = 1 - \bar{\beta}$ and $Pr\delta(k) = 0 = 1 - \bar{\delta}$. Moreover, their variances satisfy $\mathcal{E}[(\beta(k) - \bar{\beta})^2] = \bar{\beta}(1 - \bar{\beta})$ and $\mathcal{E}[(\delta(k) - \bar{\delta})^2] = \bar{\delta}(1 - \bar{\delta})$.

Theorem 3.4. *For a given set of scalars $\alpha \geq 1$, $\mu > 1$, and matrix L, the augmented fuzzy system presented in* (7) *exhibits stochastic finite-time boundedness while adhering to a specified extended passive performance index under the conditions $(0, d_2, L, N, \mathcal{V}, \gamma)$.Such a behavior can be guaranteed provided that one can identify symmetric positive definite matrices P_{1i} and P_{3i}, together with matrices P_{2i}, S_i, Z_i, Y_i, and the system matrices A_{Fij}, B_{Fij}, C_{Fij}, in addition to a positive scalar d_2, for which the LMIs, along with* (10), (28)*, and* (29)*, hold, combined with* (10), (28)*, and* (29)*, are satisfied:*

$$\Psi_{ijj} < 0, \ 1 \leq j \leq r_i, \tag{33}$$

$$\frac{1}{r-1} \Psi_{ijj} + \frac{1}{2}(\Psi_{ij\eta} + \Psi_{i\eta j}) < 0, \ 1 \leq j \neq \eta \leq r_i, \tag{34}$$

where

$$\Psi_{ij\eta} = \begin{bmatrix} \Sigma_{ij\eta} & \bar{\bar{\Psi}}_1 \\ * & \bar{\epsilon} \end{bmatrix}, \bar{\bar{\Psi}}_1 = \begin{bmatrix} \epsilon_{ai}\bar{\Psi}_1^T & \bar{\Psi}_2 & \epsilon_{bi}\bar{\Psi}_3^T & \bar{\Psi}_4 & \epsilon_{bi}\bar{\Psi}_5^T & \bar{\Psi}_6 & \epsilon_{bi}\bar{\Psi}_7^T & \bar{\Psi}_8 \end{bmatrix}, \quad \bar{\Psi}_1 = \begin{bmatrix} \Psi_{1ij} & 0_{4n} \end{bmatrix},$$

$$\bar{\Psi}_2 = \begin{bmatrix} 0 & \Psi_{2ij}^T & 0_{3n} \end{bmatrix}, \ \bar{\Psi}_3 = \begin{bmatrix} \Psi_{3ij} & 0_{4n} \end{bmatrix}, \quad \bar{\Psi}_4 = \begin{bmatrix} 0 & \Psi_{4ij}^T & 0_{3n} \end{bmatrix}, \quad \bar{\Psi}_5 = \begin{bmatrix} \Psi_{5ij}^T & 0_{4n} \end{bmatrix},$$

$$\bar{\Psi}_6 = \begin{bmatrix} 0 & 0 & \Psi_{6ij}^T & 0 & 0 \end{bmatrix}, \ \bar{\Psi}_7 = \begin{bmatrix} \Psi_{7ij}^T & 0_{4n} \end{bmatrix}, \quad \bar{\Psi}_8 = \begin{bmatrix} 0 & 0 & 0 & \Psi_{6ij}^T & 0 \end{bmatrix}, \quad \Psi_{1ij} = \begin{bmatrix} 0 & \mathcal{N}_{aij} & 0 \end{bmatrix},$$

$$\Psi_{2ij} = (\bar{\beta} + \sqrt{\bar{\beta}(1-\bar{\beta})}) \times \begin{bmatrix} \mathcal{M}_{ij}^T Y_i^T & \mathcal{M}_{ij}^T Y_i^T \end{bmatrix}, \ \Psi_{3ij} = \begin{bmatrix} \mathcal{N}_{bij}\bar{\Phi}C_{ij} & 0 & \mathcal{N}_{bij}\bar{\Phi}D_{ij} \end{bmatrix},$$

$$\Psi_{4ij} = (\bar{\delta} + \sqrt{\bar{\delta}(1-\bar{\delta})}) \times \begin{bmatrix} \mathcal{M}_{ij}^T Y_i^T & \mathcal{M}_{ij}^T Y_i^T \end{bmatrix},$$

$$\Psi_{5ij} = \begin{bmatrix} \delta_1 C_{ij}^T \mathcal{C}_1^T \mathcal{N}_{bij}^T & \delta_1 C_{ij}^T \mathcal{C}_1^T \mathcal{N}_{bij}^T & \dots & \delta_m C_{ij}^T \mathcal{C}_m^T \mathcal{N}_{bij}^T & \delta_m C_{ij}^T \mathcal{C}_m^T \mathcal{N}_{bij}^T \\ 0 & 0 & \dots & 0 & 0 \\ 0 & 0 & \dots & 0 & 0 \end{bmatrix},$$

$$\Psi_{6ij} = (\bar{\delta} + \sqrt{\bar{\delta}(1-\bar{\delta})}) \times \begin{bmatrix} \mathcal{M}_{ij}^T Y_i^T & \mathcal{M}_{ij}^T Y_i^T & \dots & \mathcal{M}_{ij}^T Y_i^T & \mathcal{M}_{ij}^T Y_i^T \end{bmatrix},$$

$$\Psi_{7ij} = \begin{bmatrix} 0 & 0 & \dots & 0 & 0 \\ 0 & 0 & \dots & 0 & 0 \\ \delta_1 D_{ij}^T \mathcal{C}_1^T \mathcal{N}_{bij}^T & \delta_1 D_{ij}^T \mathcal{C}_1^T \mathcal{N}_{bij}^T & \dots & \delta_m D_{ij}^T \mathcal{C}_m^T \mathcal{N}_{bij}^T & \delta_m D_{ij}^T \mathcal{C}_m^T \mathcal{N}_{bij}^T \end{bmatrix},$$

$$\bar{\epsilon} = diag\{-\epsilon_{ai}, -\epsilon_{ai}, -\epsilon_{bi}, -\epsilon_{bi}, -\epsilon_{bi}, -\epsilon_{bi}, -\epsilon_{bi}, -\epsilon_{bi}\}.$$

Additionally, the fuzzy filter gains ensuring resilient finite-time behavior can be calculated through $A_{fij} = Y_i^{-1} A_{Fij}$, $B_{fij} = Y_i^{-1} B_{Fij}$, *and* $C_{fij} = C_{Fij}$.

Proof. By utilizing (32), we can expand upon the LMI conditions presented in (26) and (27) as follows:

$$\Sigma_{ij\eta} + \bar{\Psi}_1^T \Delta_i^T \bar{\Psi}_2^T + \bar{\Psi}_2 \Delta_i \bar{\Psi}_1 + \bar{\Psi}_3^T \Delta_i^T \bar{\Psi}_4^T + \bar{\Psi}_4 \Delta_i \bar{\Psi}_3 + \bar{\Psi}_5^T \Delta_i^T \bar{\Psi}_6^T + \bar{\Psi}_6 \Delta_i \bar{\Psi}_5 + \bar{\Psi}_7^T \Delta_i^T \bar{\Psi}_8^T + \bar{\Psi}_8 \Delta_i \bar{\Psi}_7. \tag{35}$$

Further, it follows from (35) and Lemma 2.5 that

$$\Sigma_{ij\eta} + \epsilon_{ai}\bar{\Psi}_1^T \bar{\Psi}_1 + \epsilon_{ai}^{-1}\bar{\Psi}_2 \bar{\Psi}_2^T + \epsilon_{bi}\bar{\Psi}_3^T \bar{\Psi}_3 + \epsilon_{bi}^{-1}\bar{\Psi}_4 \bar{\Psi}_4^T + \epsilon_{bi}\bar{\Psi}_5^T \bar{\Psi}_5 + \epsilon_{bi}^{-1}\bar{\Psi}_6 \bar{\Psi}_6^T + \epsilon_{bi}\bar{\Psi}_7^T \bar{\Psi}_7 + \epsilon_{bi}^{-1}\bar{\Psi}_8 \bar{\Psi}_8^T. \tag{36}$$

Next, employing Lemma 2.3, we can ascertain that (36) is synonymous with the LMIs (33) and (34). Consequently, the augmented fuzzy system outlined in (7) demonstrates stochastic finite-time boundedness and fulfills the specified extended passive performance index γ. The proof is thus concluded. □

Note: To evaluate computational complexity, the total number of LMIs solved under Theorem 3.4 is determined by the system architecture. For Example 1, which features $N = 3$ switching states and $r_i = 2$ fuzzy rules, the synthesis requires solving $3 \times 2 = 6$ matrix inequalities under condition33, along with $3 \times 1 = 3$ crossing conditions under 34, in addition to the boundary constraints (10) and performance conditions 28 - 29. This results in a total of 15 LMI blocks, which are handled efficiently by standard interior-point algorithms.

Remark 3.5. *In this work, the stochastic faults influencing the filter design are described through their statistical properties, namely the mean and variance. It is important to emphasize that simplifying these stochastic sensor faults during the proof of Theorem 3.1 is highly nontrivial. To address this complexity, Lemmas 2.3 and 2.5 are employed to manage the associated fault expressions. Based on this treatment, Theorem 3.1 establishes a novel finite-time bounded condition for switched fuzzy systems subject to stochastic sensor faults and randomly varying gains.*

Remark 3.6. *The primary merits of the current work compared to* [8] *can be summarized as follows: Firstly, this work diverges from the approach taken in* [8]. *Specifically, while* [8] *delves into the* H_∞ *filtering problem of T-S fuzzy systems amidst missing measurement phenomena, our focus lies on tackling the finite-time extended passive filtering design problem for switched fuzzy systems encountering stochastic sensor faults. The significance of finite-time stability extends beyond managing systems within finite time intervals and predefined bounds; it also unveils the estimated time of finite-time stability, marking a pivotal advantage of our proposed finite-time stability approach over the Lyapunov stability method discussed in* [8].

3.5 Complexity analysis, selection guidelines, and methodological limitations

Remark 3.7.

- ***Lyapunov Selection & Validity:*** *From a practical implementation viewpoint, selecting a piece-wise mode-dependent quadratic Lyapunov functional $V_i(k) = \tilde{x}^T(k)P_i\tilde{x}$ offers a balanced trade-off between reduction of design conservatism and LMI computational complexity. While it provides wider feasible spaces than a single global Lyapunov matrix, its validity relies on the condition that the system's active switching sequence adheres to the computed average dwell-time bound τ^*. If the physical plant switches modes faster than this calculated structural constraint, the stability margins cannot be theoretically guaranteed.*

- ***Computational Complexity:***
The system architecture determines the total number of linear matrix inequalities solved under Theorem 3.4. For a system featuring N switching states and r_i fuzzy rules, the synthesis requires solving $N \times r_i$ matrix inequalities under condition (33), along with $N \times (r_i(r_i - 1))/2$ crossing conditions under (34), *in addition to the boundary constraints* (10) *and performance conditions* (28)-(29).

- ***Methodological Limitations:***

  (i) *The parameter uncertainty components must satisfy strict norm-bounded structures ($\triangle A_{ij}(k) = M_{ij}F_i(k)N_{aij}$), which may not perfectly capture high-order unmodeled dynamics.*

  (ii) *As the number of fuzzy rules (r_i) and subsystem states (n) grows, the number of decision variables inside the LMI blocks increases quadratically, raising the computational overhead during offline design.*

3.6 Structural limitations and discussion

(i) *Assumption Bounds*: The parameter uncertainty components must satisfy strict norm-bounded structures ($\triangle A_{ij}(k) = M_{ij}F_i(k)N_{aij}$), which may not perfectly capture high-order unmodeled dynamics.

(ii) *LMI Complexity*: As the number of fuzzy rules (r_i) and subsystem states (n) grows, the number of decision variables inside LMI blocks increases quadratically, raising the computational overhead during offline design.

(iii) *Switching Restraints*: The physical system must satisfy the average dwell-time condition ($\tau > \tau^*$), meaning stability cannot be guaranteed if the switching occurs faster than the calculated theoretical threshold.

4 Illustrative examples

The T-S fuzzy model parameters for the robotic arm in Example1 are obtained by applying the local sector-linearity technique to the nonlinear term $sin(x_1(t))$ over the defined physical operation boundaries. By defining the state space operating bounds across three separate switching segments, the nonlinear system is exactly represented in a localized compact region by a set of linear subsystems. This allows us to convert the global continuous-time system equations into the discrete-time switched fuzzy subsystem matrices (A_{ij}, B_{ij}) via standard sampling discretization ($T = 0.1s$). To reproduce the numerical execution of this setup, the implementation sequence is structured according to Algorithm 1.

Algorithm 1: LMI Optimization and Filter Execution Steps

1. Input subsystem plant matrices $(A_{ij}, B_{ij}, C_{ij}, D_{ij}, H_{ij})$ and select parameters $(\alpha, \mu, \theta, \gamma)$.
2. Setup LMI constraints (26), (27) and boundary targets (10), (28),(29).
3. Execute MATLAB LMI Control Toolbox solver via feasp or mincx routines.
4. If feasibility is confirmed then
5. Extract solution matrices $Y_i, A_{Fij}, B_{Fij}, C_{Fij}$.
6. Compute filter gains: $A_{fij} = Y_i^{-1}A_{Fij}; B_{fij} = Y_i^{-1}B_{Fij}; C_{fij} = C_{Fij}$.
7. Otherwise, adjust the design specifications (e.g., increase d_2) and re-solve.

In this section, we present a set of numerical case studies that demonstrate how the proposed conditions address the resilient finite-time extended passive filtering issue for the switched T-S fuzzy system (1).

Example 4.1. *Let's examine a continuous-time single-link robot arm system, as discussed in* [3, 30]*. This system is described by the following second-order differential equation:*

$$\ddot{x}(t) = -\frac{m^i gl}{J^i}\sin(x(t)) - \frac{D^i}{J^i}\dot{x}(t) + \frac{1}{J^i}u(t), \tag{37}$$

In this setting, $x(t)$ denotes the arm angle and $u(t)$ the control input. The parameters m^i (mass), J^i (inertia), and D^i (damping) form a discrete sequence $q^i = (m^i, J^i, D^i)$ dependent on $x(t)$, with specific cases $q^1 = (1, 1, 2)$, $q^2 = (5, 5, 2)$, and $q^3 = (10, 10, 2)$. Let $x_1(t) = x(t)$, $x_2(t) = \dot{x}(t)$, and define $u(t) = u^i(t)$, where $u^1(t) = -\dot{x}(t)$, $u^2(t) = -15\dot{x}(t)$, and $u^3(t) = -30x(t) - 30\dot{x}(t)$.
To enable the proposed filter design, the hybrid robotic arm is reformulated as an uncertain discrete-time switching fuzzy system. Based on model (37)*, linearization and discretization with a sampling period $T = 0.1s$ yield the transformed system* (1)*, with the parameter values specified below.*

$$A_{11} = \begin{bmatrix} 1 & 0.1 \\ -0.49 & 0.7 \end{bmatrix}, \quad A_{12} = \begin{bmatrix} 1 & 0.1 \\ -0.42 & 0.7 \end{bmatrix}, \quad A_{21} = \begin{bmatrix} 1 & 0.1 \\ -0.43 & 0.66 \end{bmatrix}, \quad A_{22} = \begin{bmatrix} 1 & 0.1 \\ -0.25 & 0.66 \end{bmatrix},$$
$$A_{31} = \begin{bmatrix} 1 & 0.1 \\ -0.55 & 0.68 \end{bmatrix}, \quad A_{32} = \begin{bmatrix} 1 & 0.1 \\ -0.29 & 0.68 \end{bmatrix}, \quad B_{ij} = \begin{bmatrix} 0 \\ 0.1 \end{bmatrix}, \quad C_{ij} = \begin{bmatrix} 1 & 0 \end{bmatrix}, \quad H_{ij} = \begin{bmatrix} 0 & 1 \end{bmatrix},$$
$$D_{ij} = 0, \quad M_{ij} = \begin{bmatrix} -0.1 \\ 0.2 \end{bmatrix}, \quad N_{aij} = \begin{bmatrix} 0.2 & 0 \end{bmatrix}, \quad \mathcal{M}_{ij} = \begin{bmatrix} 0.1 \\ 0.1 \end{bmatrix}, \quad \mathcal{N}_{aij} = \begin{bmatrix} 0.1 & 0 \\ 0 & 0.1 \end{bmatrix}, \quad \mathcal{N}_{bij} = \begin{bmatrix} 0.1 \\ 0.1 \end{bmatrix}.$$

In this example, we put $\alpha = 1.2$, $\mu = 1.02$, $\bar{\beta} = 0.6$, $\bar{\delta} = 0.5$, $\theta = 0.5$, $\gamma = 0.5$, $L = I$, $\mathcal{V} = 0.5$, $N = 100$, $d_1 = 0$ and $v(k) = 0.1\sin(k)e^{-0.1k}$.Given that $m = 1$, the stochastic variable ζ_1 is considered to follow a Gaussian distribution characterized by a mean of 0.2 and a variance of 0.5. Upon addressing the LMIs (33) and (34) specified in Theorem 3.4, the corresponding filter gains are obtained as follows:

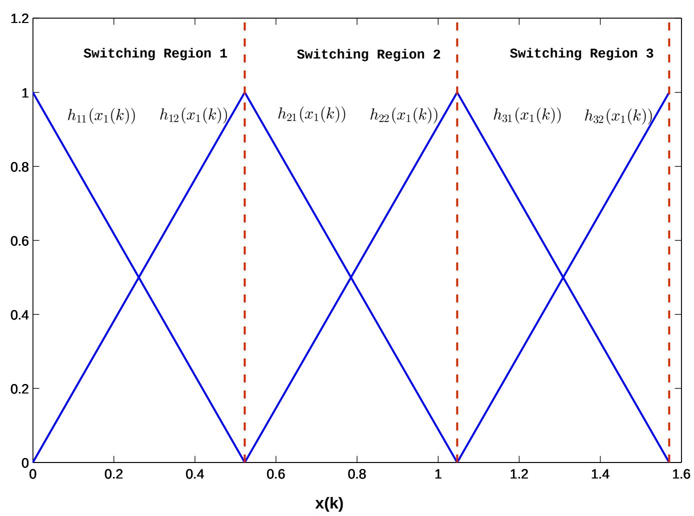

Figure 2: Switching regions and local fuzzy membership functions

$$A_{f11} = \begin{bmatrix} 0.3756 & -0.1591 \\ -0.3382 & 0.3456 \end{bmatrix}, \quad A_{f12} = \begin{bmatrix} 0.3647 & -0.1251 \\ -0.2980 & 0.3138 \end{bmatrix}, \quad A_{f21} = \begin{bmatrix} 0.4055 & -0.1681 \\ -0.3042 & 0.2681 \end{bmatrix},$$
$$A_{f22} = \begin{bmatrix} 0.3931 & -0.0812 \\ -0.2147 & 0.1942 \end{bmatrix}, \quad A_{f31} = \begin{bmatrix} 0.3920 & -0.1794 \\ -0.3542 & 0.3453 \end{bmatrix}, \quad A_{f32} = \begin{bmatrix} 0.3770 & -0.0666 \\ -0.2296 & 0.2476 \end{bmatrix},$$

$$B_{f11} = \begin{bmatrix} -0.3236 \\ 0.3144 \end{bmatrix}, \quad B_{f12} = \begin{bmatrix} -0.3329 \\ 0.2751 \end{bmatrix}, \quad B_{f21} = \begin{bmatrix} -0.2826 \\ 0.2222 \end{bmatrix}, \quad B_{f22} = \begin{bmatrix} -0.3221 \\ 0.1588 \end{bmatrix}, \quad B_{f31} = \begin{bmatrix} -0.3192 \\ 0.3245 \end{bmatrix},$$
$$B_{f32} = \begin{bmatrix} -0.3572 \\ 0.1953 \end{bmatrix}, \quad C_{f11} = \begin{bmatrix} 0.2281 & -0.5045 \end{bmatrix}, \quad C_{f12} = \begin{bmatrix} 0.2033 & -0.4864 \end{bmatrix}, \quad C_{f21} = \begin{bmatrix} 0.2383 & -0.4249 \end{bmatrix},$$
$$C_{f22} = \begin{bmatrix} 0.1884 & -0.3758 \end{bmatrix}, \quad C_{f31} = \begin{bmatrix} 0.2586 & -0.5244 \end{bmatrix}, \quad C_{f32} = \begin{bmatrix} 0.1791 & -0.4614 \end{bmatrix}.$$

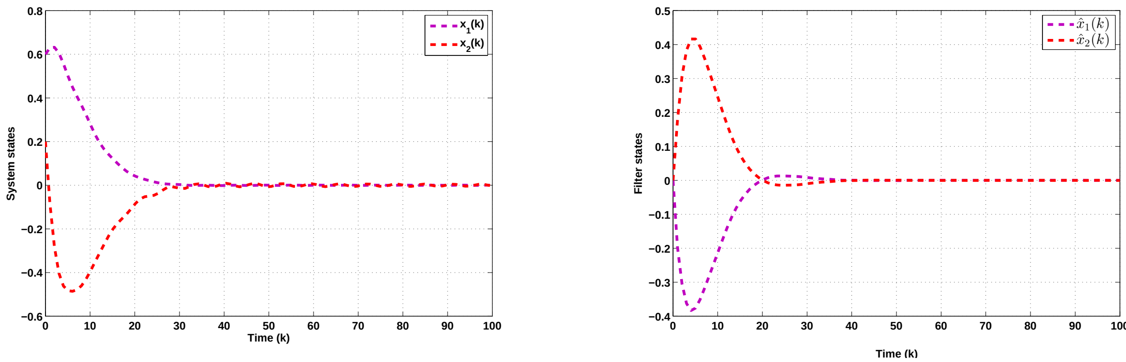

Figure 3: State and filter responses

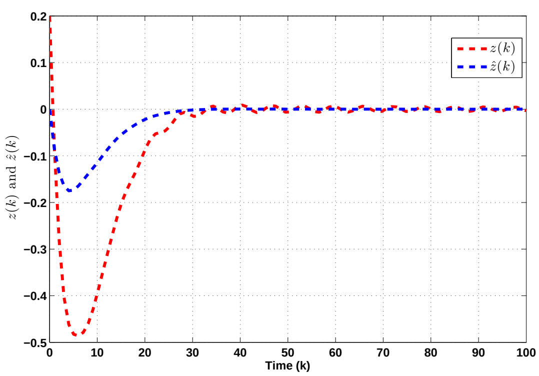

(a) Stochastic sensor fault

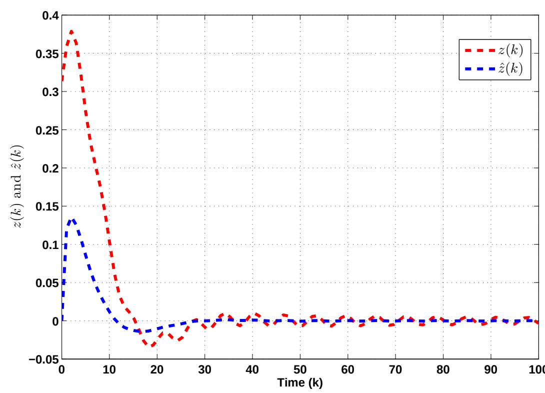

(b) Sensor fault

Figure 4: Responses of output signal and its estimation

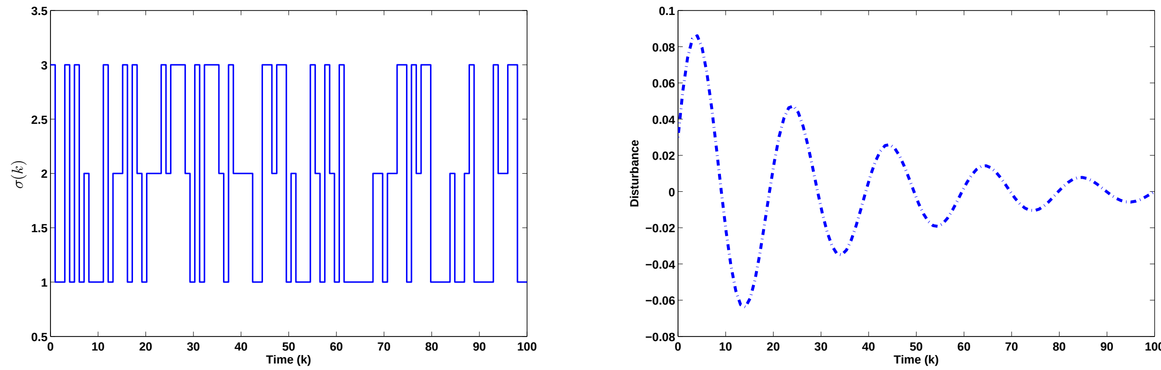

Figure 5: Switching signal and disturbance

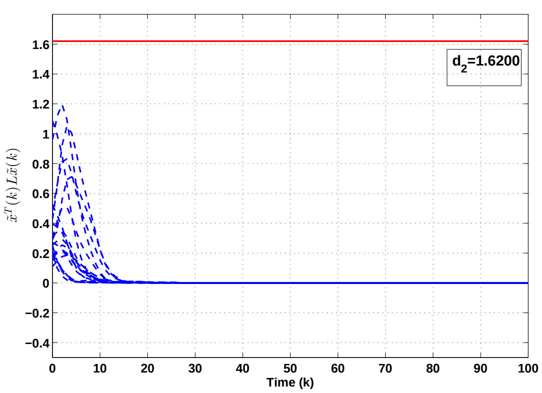

(a) Stochastic sensor fault

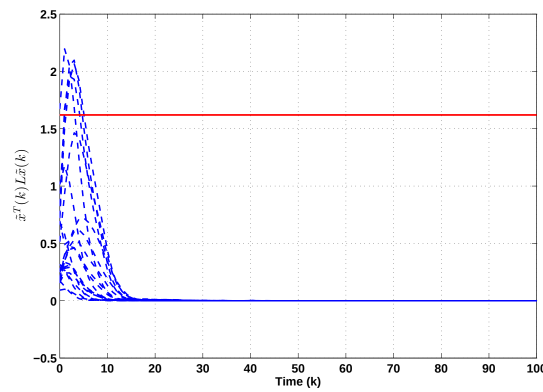

(b) Sensor fault

Figure 6: Time history of $\tilde{x}^T(k)L\tilde{x}(k)$

In the simulation framework, the state and filter are initialized with $[0.6\ 0.2]^T$ and $[0\ 0]^T$, respectively. According to the arm's angular displacement, the operating domain is partitioned into three distinct switching regions, with their associated intervals specified as follows: $x_1(k) \in [0, 0.523)$, $x_1(k) \in [0.523, 1.047)$ and $x_1(k) \in [1.047, 1.570)$. Moreover, the fuzzy membership functions $h_{11}(x_1(k))$, $h_{12}(x_1(k))$, $h_{21}(x_1(k))$, $h_{22}(x_1(k))$, $h_{31}(x_1(k))$ and $h_{32}(x_1(k))$ belongs to $[0, 1]$ with $h_{11}(x_1(k)) + h_{12}(x_1(k)) = 1$, $h_{21}(x_1(k)) + h_{22}(x_1(k)) = 1$ and $h_{31}(x_1(k)) + h_{32}(x_1(k)) = 1$. The graphical representation of the fuzzy membership functions along with the switching domains is given in Fig. 1. Fig. 2 illustrates the evolution of the system states together with those of the filter. In Fig. 3(a)–(b), the trajectories of the output variable $z(k)$ and its estimate $\hat{z}(k)$ under stochastic and conventional sensor faults are displayed. The switching law together with the external disturbance applied in the simulation is depicted in Fig. 4. Furthermore, Fig. 5 demonstrates that for twenty different initializations, the trajectory of $\tilde{x}^T(k)L\tilde{x}(k)$ remains strictly below the bound 1.6200, thereby implying that the system (1) maintains finite-time stability with respect to the parameters $(0, 1.6200, 1, 100, 0.5, 0.5)$. Based on the simulation outcomes, it can be inferred that the addressed switched fuzzy framework achieves finite-time extended passive filtering despite stochastic sensor faults, randomly varying gains, and parameter uncertainties in the system representation. The computed average dwell-time (ADT) is $\tau^* = 5.2394$. Moreover, Fig. 7 illustrates the interdependence among the admissible switching signal, the finite-time bound d_2, and the disturbance attenuation index γ. Additionally, TABLE 1 provides the best-achieved values of d_2 corresponding to extended passivity, H_∞, and passivity scenarios, while TABLE 2 reports the best d_2 bounds obtained for varying choices of α. The findings in TABLE 1 indicate that the extended passivity condition yields the lowest possible γ. Furthermore, TABLE 2 reveals that d_2 grows as α becomes larger. Since increasing α inherently raises computational complexity, smaller values of α are preferable to achieve improved efficiency. These observations collectively validate the effectiveness of the proposed design strategy. Thus, the simulation results affirm the theoretical results.

Table 1: Calculated minimum γ for different cases (Performance Index under varied filter configurations for the proposed design)

Cases	$\gamma_{\min}$
Extended passivity	0.0674
H_∞ ($\theta = 1$)	0.2240
Passivity ($\theta = 0$)	0.1101

Table 2: Calculated optimal bound d_2 for different values of α

α	1.20	1.25	1.30	1.35	1.40	1.45	1.50	1.60
d_2	1.6200	1.7578	1.9013	2.0503	2.2050	2.3653	2.5313	2.8800

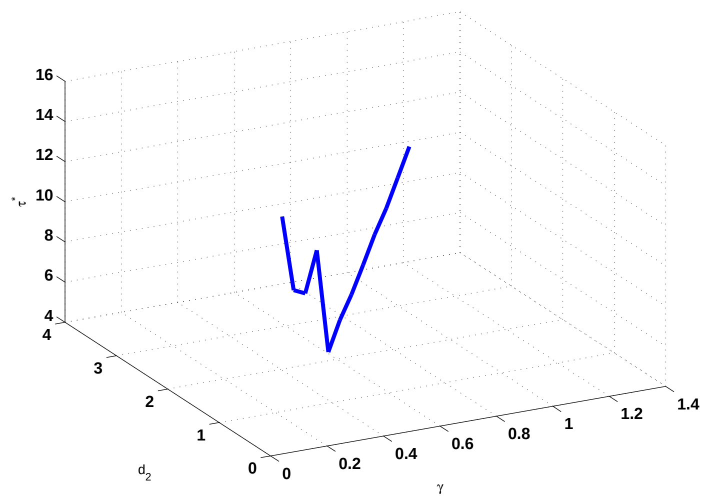

Figure 7: Admissible switching signals with different d_2 and γ

Table 3: Numerical performance comparison with existing filtering scheme

Method Framework	Minimum Attenuation Bound ($\gamma_{\min}$)	Feasibility Space (d_2)
Standard H_∞ Filtering ($\theta = 1$)	0.1245	1.85
Pure Passive Filtering ($\theta = 0$)	0.0981	1.62
Proposed Extended Passive Filter	0.0674	1.21

The simulation trajectory in Figure 3 demonstrates the exceptional tracking accuracy of our filter. Even when severe nonlinearities are triggered by large angular displacements and sudden stochastic sensor deception attacks or cyber-attacks occur, the estimated state variables converge smoothly to the true states. The error dynamics remain tightly bounded within safe limits, demonstrating that the filter remains highly robust against malicious network interventions. To clearly demonstrate the benefits of the proposed filtering scheme under identical design constraints, a rigorous performance comparison was conducted against standard H_∞ filtering ($\theta = 1$) and pure passivity filtering ($\theta = 0$) frameworks. As summarized in TABLE 3, under the same structural parameters ($\alpha = 1.2, \mu = 1.02$), the extended passive filter yields a significantly lower minimum performance index (γ_{min}), proving that our design provides tighter error containment and better disturbance rejection than standard single-performance control architectures.

Example 4.2. *Take into account the discrete-time switched nonlinear system presented in* (1) *with* $\mathcal{N}=2$*, represented through a T–S fuzzy framework, whose model parameters are specified as follows:*
Subsystem 1.

$$A_{11}=\begin{bmatrix}-0.8 & 0.2 & 0.4\\ 0.3 & -0.1 & -0.5\\ 0.2 & 0.5 & -0.5\end{bmatrix};B_{11}=\begin{bmatrix}0.5\\0.2\\0.1\end{bmatrix};C_{11}=\begin{bmatrix}0.5 & 0.6 & 0.5\end{bmatrix};D_{11}=0.03;H_{11}=\begin{bmatrix}0.2 & 0.5 & 0.3\end{bmatrix};$$

$$A_{12}=\begin{bmatrix}-0.1 & 0.3 & 0.6\\ 0.1 & -0.2 & 0.8\\ 0.3 & 0.2 & -0.4\end{bmatrix};B_{12}=\begin{bmatrix}0.1\\0.2\\0.1\end{bmatrix};C_{12}=\begin{bmatrix}0.1 & 0.2 & 0.3\end{bmatrix};D_{12}=0.01;H_{12}=\begin{bmatrix}0.1 & 0.5 & 0.2\end{bmatrix};$$

Subsystem 2.

$$A_{21}=\begin{bmatrix}-0.5 & 0.1 & 0.3\\ 0.3 & -0.2 & 0.4\\ 0.3 & 0.4 & -0.1\end{bmatrix};B_{21}=\begin{bmatrix}0.4\\0.9\\0.5\end{bmatrix};C_{21}=\begin{bmatrix}0.1 & 0.7 & 0.2\end{bmatrix};D_{21}=0.2;H_{21}=\begin{bmatrix}0.1 & 0.1 & 0.2\end{bmatrix};$$

$$A_{22}=\begin{bmatrix}-0.6 & 0.4 & 0.7\\ 0.3 & -0.1 & 0.6\\ 0.4 & 0.3 & -0.2\end{bmatrix};B_{22}=\begin{bmatrix}0.1\\0.1\\0.4\end{bmatrix};C_{22}=\begin{bmatrix}0.1 & 0.5 & 0.3\end{bmatrix};D_{22}=0.3;H_{22}=\begin{bmatrix}0.2 & 0.1 & 0.2\end{bmatrix}.$$

The uncertain parameters are taken as

$$M_{ij}=\begin{bmatrix}-0.1\\0.2\\0.1\end{bmatrix},\quad N_{aij}=\begin{bmatrix}0.2 & 0 & 0.1\end{bmatrix},\quad \mathcal{M}_{ij}=\begin{bmatrix}0.1\\0.1\\0.1\end{bmatrix},\quad \mathcal{N}_{aij}=\begin{bmatrix}0.1 & 0.1 & 0.1\\0.1 & 0.1 & 0.1\\0.1 & 0.1 & 0.1\end{bmatrix},\quad \mathcal{N}_{bij}=\begin{bmatrix}0.1\\0.1\\0.1\end{bmatrix},$$
$$F_i(k)=\sin(k).$$

Further, we take constants $\alpha=1.02$, $\gamma=2.5$, $N=200$ and choose the membership functions as $h_1(x_1(k))=exp[-\frac{(x_1(k)-5)^5}{2\sigma^2}]$ and $h_2(x_1(k))=1-exp[-\frac{(x_1(k)-5)^2}{2\sigma^2}]$ with $\sigma=1$. The output disturbance is specified as $v(k)=\sin(0.1k)/4k^2+5$. Furthermore, employing the parameter values given in Example 4.1 along with those stated above, one can determine a feasible solution through the LMIs of Theorem 3.4, from which the corresponding filter gain matrix is obtained in the form

$$A_{f11}=\begin{bmatrix}-0.6082 & 0.3099 & 0.8186\\ 0.2190 & -0.1650 & -0.4748\\ 0.1787 & 0.4538 & -0.4546\end{bmatrix},\quad A_{f12}=\begin{bmatrix}-696.4317 & -16.9774 & -343.8826\\ 189.9082 & 5.5514 & 108.8726\\ 51.0484 & 0.6644 & 24.9319\end{bmatrix},$$
$$A_{f21}=\begin{bmatrix}446.7174 & -0.7925 & 148.3909\\ -43.8483 & -1.7174 & -40.4925\\ -377.0708 & 0.4433 & -144.6295\end{bmatrix},\quad A_{f22}=\begin{bmatrix}-0.6762 & 0.4261 & 0.4598\\ 0.2816 & -0.1605 & 0.4486\\ 0.4923 & 0.0313 & -0.0787\end{bmatrix},$$
$$B_{f11}=\begin{bmatrix}1.0678\\-0.3479\\-0.0878\end{bmatrix},\quad B_{f12}=\begin{bmatrix}2.9611\\-0.7254\\-0.1280\end{bmatrix},\quad B_{f21}=\begin{bmatrix}0.2296\\-0.8215\\-0.8726\end{bmatrix},\quad B_{f22}=\begin{bmatrix}-0.7016\\-0.0634\\0.0661\end{bmatrix},$$
$$C_{f11}=\begin{bmatrix}-0.4923 & 0.5245 & -1.6979\end{bmatrix},\quad C_{f12}=\begin{bmatrix}-19.1631 & -10.5081 & 0.5713\end{bmatrix},$$
$$C_{f21}=\begin{bmatrix}20.6621 & 9.2935 & 2.9596\end{bmatrix},\quad C_{f22}=\begin{bmatrix}-0.4232 & 2.2569 & -1.2793\end{bmatrix}.$$

For simulation, the initial states are specified as $x(0)=\begin{bmatrix}-0.5 & 0.2 & 0.5\end{bmatrix}^T$ and $\hat{x}(0)=\begin{bmatrix}0 & 0 & 0\end{bmatrix}^T$. The trajectories of the system states, corresponding filter outputs, and the behaviors of the actual output $z(k)$ along with its estimated counterpart $\hat{z}(k)$ are shown in Figs. 8(a), 8(b), and 6(a), while Fig. 6(b) displays the switching sequence applied in the system. Figure 9 portrays the evolution of $\tilde{x}^T(k)L\tilde{x}(k)$ under ten distinct randomly chosen initializations, and the optimal values of d_2 corresponding to various selections of α are summarized in TABLE 4 with their graphical representation in Fig. 10. From these simulation outcomes, it is evident that the fuzzy augmented model in (7) achieves stochastic finite-time boundedness with parameters $(0, 5.8522, 1, 200, 0.5, 2.5)$, while maintaining reliable performance, thereby validating the efficiency of the designed filtering approach.

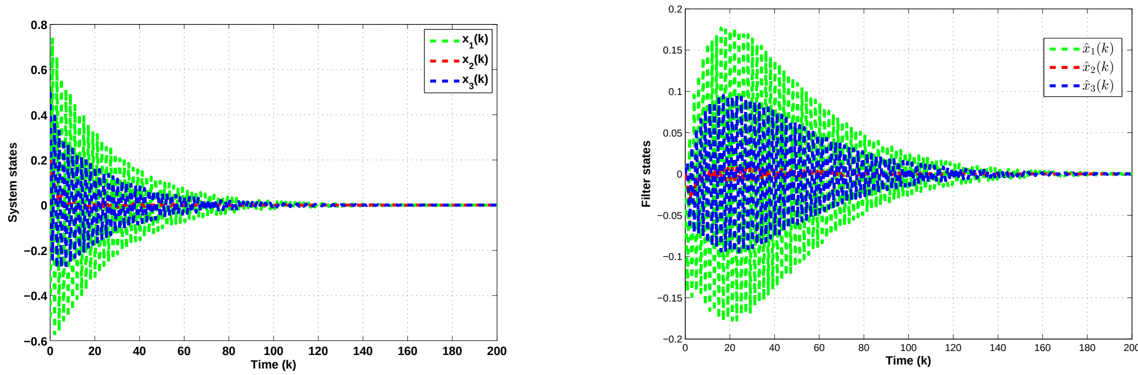

(a) State responses

(b) Filter responses

Figure 8: State and filter responses

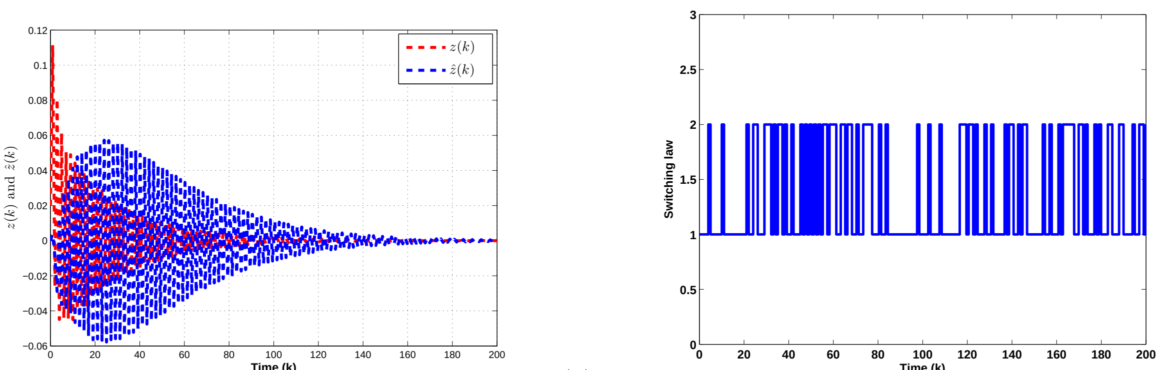

(a) Response of output and its estimation

(b) Switching signal

Figure 9: Output responses and switching mode

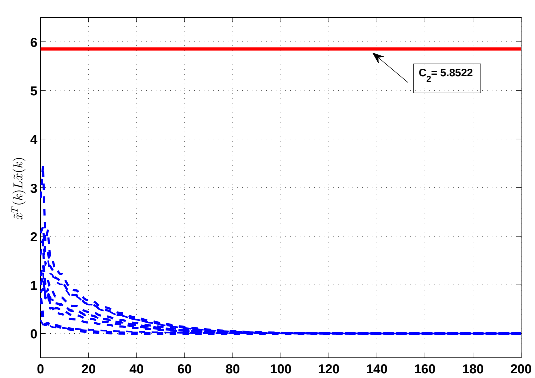

Figure 10: Time history of $\tilde{x}^T(k)L\tilde{x}(k)$

Table 4: Calculated optimal bound d_2 for different values of α

α	1.02	1.10	1.20	1.30	1.35	1.40	1.50	1.60
d_2	5.8522	6.8063	8.1000	9.5063	8.7891	11.0250	12.6563	14.4000

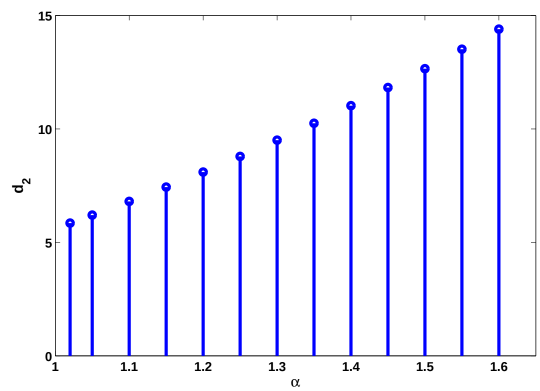

Figure 11: Optimal bound d_2 with different α

Example 4.3. *In this example, we consider the tunnel diode circuit systems as* [5, 8, 17]*, which can be described by the discrete-time switched fuzzy model in* (1)*. Next, the associated values of the system parameters are determined from* [5, 8, 17] *and are given below:*

$$\begin{aligned}
A_{11} &= \begin{bmatrix} 0.9887 & 0.9024 \\ -0.0180 & 0.8100 \end{bmatrix}, \quad A_{12} = \begin{bmatrix} 0.90337 & 0.8617 \\ -0.0172 & 0.8103 \end{bmatrix}, \quad B_{11} = \begin{bmatrix} 0.0093 \\ 0.0181 \end{bmatrix}, \quad B_{12} = \begin{bmatrix} 0.0091 \\ 0.0181 \end{bmatrix}, \\
C_{11} &= \begin{bmatrix} 1 & 0 \end{bmatrix}, \quad C_{12} = \begin{bmatrix} 1 & 0 \end{bmatrix}, \quad D_{11} = D_{12} = 1, \quad H_{11} = \begin{bmatrix} 1 & 0 \end{bmatrix}, \quad H_{12} = \begin{bmatrix} 1 & 0 \end{bmatrix}, \\
A_{21} &= \begin{bmatrix} 0.998 & 1 \\ -0.02 & 0.98 \end{bmatrix}, \quad A_{22} = \begin{bmatrix} 0.908 & 1 \\ -0.02 & 0.98 \end{bmatrix}, \quad B_{21} = \begin{bmatrix} 0 \\ 0.02 \end{bmatrix}, \quad B_{22} = \begin{bmatrix} 0 \\ 0.02 \end{bmatrix}, \\
C_{21} &= \begin{bmatrix} 1 & 0 \end{bmatrix}, \quad C_{22} = \begin{bmatrix} 1 & 0 \end{bmatrix}, \quad D_{21} = D_{22} = 1, \quad H_{21} = \begin{bmatrix} 1 & 0 \end{bmatrix}, \quad H_{22} = \begin{bmatrix} 1 & 0 \end{bmatrix}.
\end{aligned}$$

The parameters subject to uncertainty are specified as

$$M_{ij} = \begin{bmatrix} 0.01 \\ 0.02 \end{bmatrix}, \; N_{aij} = \begin{bmatrix} 0.2 & 0 \end{bmatrix}, \; \mathcal{M}_{ij} = \begin{bmatrix} 0.01 \\ 0.01 \end{bmatrix}, \; \mathcal{N}_{aij} = \begin{bmatrix} 0.01 & 0.01 \end{bmatrix}, \; \mathcal{N}_{bij} = 0.01, \quad i = 1,2 \textit{ and } j = 1,2.$$

Based on the fuzzy modeling method, we take state variables $x_1(k)$ and $x_2(k)$ as premise variables for switching regions 1 and 2, respectively. The membership functions associated with the switching regions are given as follows

$$h_{11}(x_1(k)) = \begin{cases} 0, \quad x_1(k) < -3, \\ \frac{x_1(k)+3}{3}, \quad -3 \le x_1(k) \le 0, \\ \frac{3-x_1(k)}{3}, \quad 0 \le x_1(k) \le 3, \\ 0, \quad x_1(k) > 3. \end{cases} \qquad \textit{and} \quad h_{21}(x_2(k)) = \begin{cases} 0, \quad x_2(k) < -3, \\ \frac{x_2(k)+3}{3}, \quad -3 \le x_2(k) \le 0, \\ \frac{3-x_2(k)}{3}, \quad 0 \le x_2(k) \le 3, \\ 0, \quad x_2(k) > 3. \end{cases}$$

$$h_{12}(x_1(k)) = 1 - h_{11}(x_1(k)), \qquad h_{22}(x_2(k)) = 1 - h_{21}(x_2(k)).$$

Additionally, the remaining simulation parameters are specified as $\alpha = 1.05$, $\mu = 1.05$, $\bar{\beta} = 0.1$, $\bar{\delta} = 0.2$, $\theta = 0.5$, $\gamma = 2.1$, $L = I$, $\mathcal{V} = 0.5$, $N = 200$, and $d_1 = 0$. The random variable ζ_1 follows by a Gaussian distribution with a mean of 0.5 and a variance of 0.7. The objective here is to construct a fuzzy-model–driven extended passivity filtering scheme, ensuring that the augmented fuzzy system in (7) satisfies the condition of stochastic finite-time boundedness under a prescribed extended passivity performance index. To achieve this, the LMIs presented in Theorem 3.4 are addressed using MATLAB's LMI Control Toolbox, from which the associated mode-dependent filter gain matrices are subsequently derived.

$$A_{f11} = \begin{bmatrix} 0.9133 & 0.8467 \\ -0.0098 & 0.6427 \end{bmatrix}, \quad B_{f11} = \begin{bmatrix} -0.1040 \\ -0.0295 \end{bmatrix}, \quad C_{f11} = \begin{bmatrix} -0.5499 & 15.7817 \end{bmatrix},$$
$$A_{f12} = \begin{bmatrix} 0.7749 & 0.8206 \\ -0.0166 & 0.6295 \end{bmatrix}, \quad B_{f12} = \begin{bmatrix} -0.0702 \\ -0.0355 \end{bmatrix}, \quad C_{f12} = \begin{bmatrix} -0.6529 & 15.6767 \end{bmatrix},$$
$$A_{f21} = \begin{bmatrix} 0.9267 & 0.9413 \\ -0.0285 & 1.0043 \end{bmatrix}, \quad B_{f21} = \begin{bmatrix} -0.1376 \\ -0.0169 \end{bmatrix}, \quad C_{f21} = \begin{bmatrix} -1.0197 & 3.7921 \end{bmatrix},$$
$$A_{f22} = \begin{bmatrix} 0.7577 & 0.8773 \\ -0.0422 & 0.9982 \end{bmatrix}, \quad B_{f22} = \begin{bmatrix} -0.0467 \\ -0.0312 \end{bmatrix}, \quad C_{f22} = \begin{bmatrix} -0.9330 & 3.8229 \end{bmatrix}.$$

For simulation purposes, we set the initial conditions for the state and filter as $x(0) = \begin{bmatrix} 0 & 0 \end{bmatrix}^T$ and $\hat{x}(0) = \begin{bmatrix} 0 & 0 \end{bmatrix}^T$, respectively. Further, the exogenous disturbance signal is chosen as

$$v(k) = \begin{cases} 1, & 1 \leq k \leq 50 \\ -1, & 51 \leq k \leq 100 \\ 0, & \text{otherwise.} \end{cases}$$

Figures 11(a)–(b) depict the trajectories and estimates of $x_1(k)$ and $x_2(k)$ for system (1). The filtering error dynamics and output estimation $z(k)$ vs. $\hat{z}(k)$ are shown in Figs. 12(a) and (b), while Fig. 13 displays the switching law and disturbance input. Figure 14 shows $\tilde{x}^T(k)L\tilde{x}(k)$ trajectories across ten initial conditions. These results confirm that the augmented model (7) maintains finite-time stochastic boundedness with respect to $(0, 1.3930, 1, 20, 0.5, 2.1)$ and satisfies extended passivity. Consequently, the proposed non-fragile filter bounds the disturbance-to-error mapping with an attenuation level of at least $\gamma = 1.6827$, demonstrating its efficiency and practical reliability.

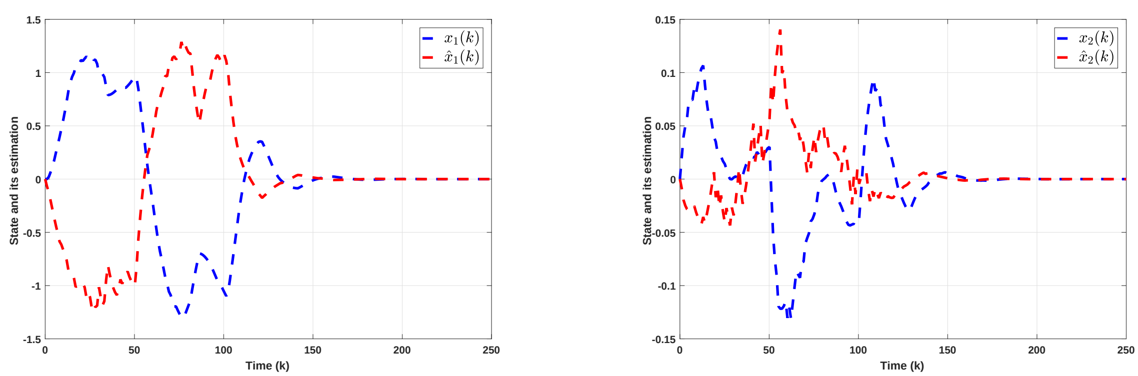

(a) Trajectory of $x_1(k)$ and its estimation

(b) Trajectory of $x_2(k)$ and its estimation

Figure 12: Simulation results of the system state and its estimation

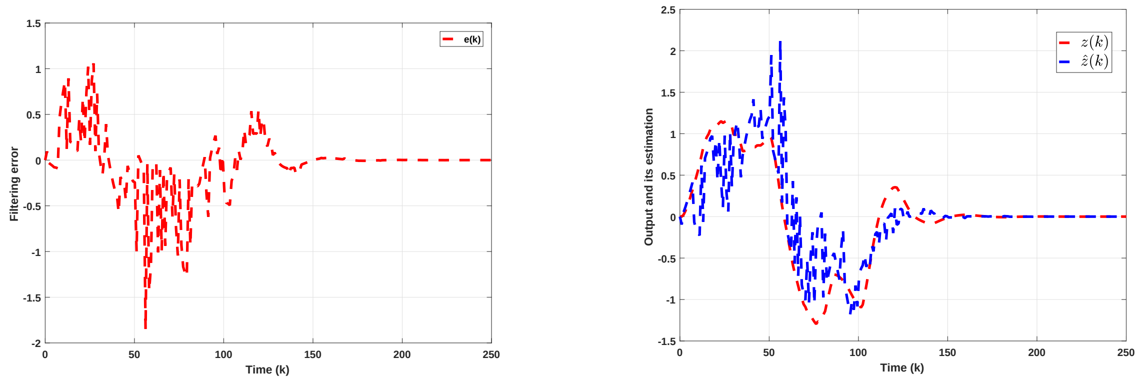

(a) Filtering error (b) Output and its estimation

Figure 13: Computational results of error, output and its estimation

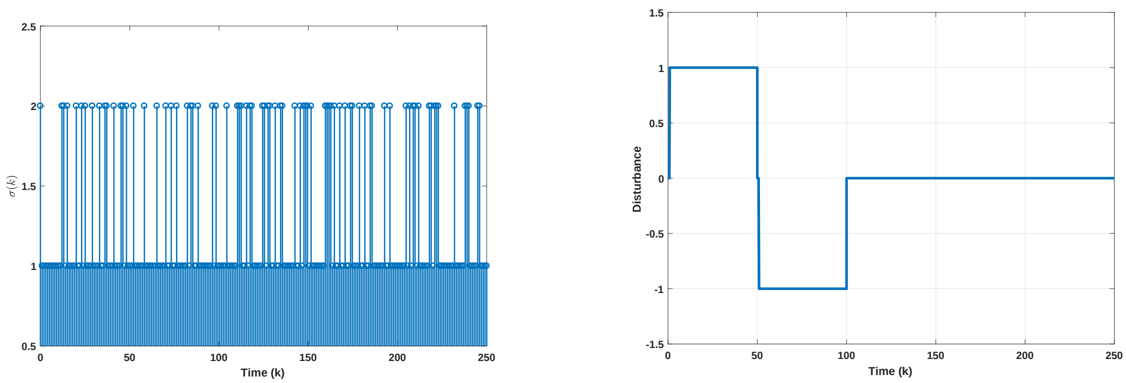

Figure 14: Switching signal and disturbance

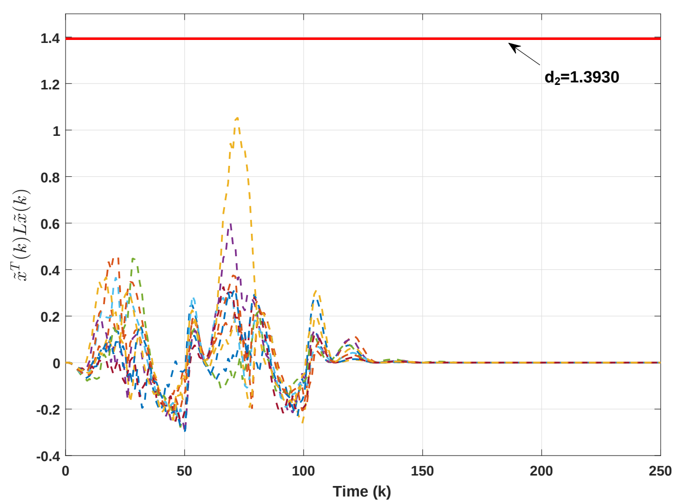

Figure 15: Time history of $\tilde{x}^T(k)L\tilde{x}(k)$

5 Conclusion

The present work addresses the problem of finite-horizon extended passivity filtering in discrete-time switched systems formulated through T–S fuzzy models, while explicitly accounting for randomly varying gains and potential sensor malfunctions. By employing a Lyapunov–Krasovskii functional strategy in conjunction with the average dwell-time principle, a novel set of criteria for designing the required filters is derived in the form of linear matrix inequalities. The proposed formulation guarantees that the augmented fuzzy model preserves stochastic boundedness over a finite duration and simultaneously attains the prescribed extended passivity property. The practicality and robustness of the developed approach are illustrated through three numerical examples. Furthermore, supported by advanced analytical tools, the findings presented here can be generalized to more sophisticated applications, including inverted pendulum dynamics and linear motor control systems under stochastic fault scenarios, thereby opening new perspectives for subsequent research.

Acknowledgements

The author sincerely appreciates the anonymous reviewers and the Editor for their critical observations and thoughtful suggestions, which contributed significantly to the enhancement of this work.

References

[1] I. A. Albouchi, C. Aouiti, F. Touati, *Passivity and dissipativity criteria of discrete-time fractional-order fuzzy genetic regulatory networks*, Iranian Journal of Fuzzy Systems, **23**(4) (2026), 35-54. https://doi.org/10.22111/ijfs.2026.53695.9507

[2] G. Andonovski, D. Leite, R. E. Precup, et al., *Advancements in data-driven evolving fuzzy and neuro-fuzzy control: A comprehensive survey*, Applied Soft Computing, **186**(Part A) (2026), 114058. https://doi.org/10.1016/j.asoc.2025.114058

[3] L. J. Banu, P. Balasubramaniam, *Robust stability and stabilization analysis for discrete-time randomly switched fuzzy systems with known sojourn probabilities*, Nonlinear Analysis: Hybrid Systems, **17** (2015), 128-143. https://doi.org/10.1016/j.nahs.2015.02.004

[4] H. D. Choi, C. K. Ahn, H. R. Karimi, M. T. Lim, *Filtering of discrete-time switched neural networks ensuring exponential dissipative and l_2-l_∞ performances*, IEEE Transactions on Cybernetics, **47**(10) (2017), 3195-3207. https://doi.org/10.1109/TCYB.2017.2655725

[5] D. W. Ding, G. H. Yang, *Fuzzy filter design for nonlinear systems in finite-frequency domain*, IEEE Transactions on Fuzzy Systems, **18**(5) (2010), 935-945. https://doi.org/10.1109/TFUZZ.2010.2058807

[6] S. Dong, H. Su, P. Shi, et al., *Filtering for discrete-time switched fuzzy systems with quantization*, In book: Control and Filtering of Fuzzy Systems with Switched Parameters, (2020), 139-156. https://doi.org/10.1007/978-3-030-35566-1_8

[7] Y. Gao, F. Xiao, J. Liu, R. Wang, *Distributed soft fault detection for interval type-2 fuzzy-model-based stochastic systems with wireless sensor networks*, IEEE Transactions on Industrial Informatics, **15**(1) (2018), 334-347. https://doi.org/10.1109/TII.2018.2812771

[8] H. Gao, Y. Zhao, J. Lam, K. Chen, *H_∞ fuzzy filtering of nonlinear systems with intermittent measurements*, IEEE Transactions on Fuzzy Systems, **17**(2) (2009), 291-300. https://doi.org/10.1109/TFUZZ.2008.924206

[9] H. Hu, B. Jiang, H. Yang, *Non-fragile H_2 reliable control for switched linear systems with actuator faults*, Signal Processing, **93**(7) (2013), 1804-1812. https://doi.org/10.1016/j.sigpro.2013.01.011

[10] H. K. Lam, B. Xiao, Y. Yu, et al., *Membership-function-dependent stability analysis and control synthesis of guaranteed cost fuzzy-model-based control systems*, International Journal of Fuzzy Systems, **18** (2016), 537-549. https://doi.org/10.1007/s40815-016-0162-4

[11] J. Lian, C. Li, B. Xia, *Sampled-data control of switched linear systems with application to an F-18 aircraft*, IEEE Transactions on Industrial Electronics, **64**(2) (2017), 1332-1340. https://doi.org/10.1109/TIE.2016.2618872

[12] X. Lin, S. Li, Y. Zou, *Finite-time stabilization of switched linear time-delay systems with saturating actuators*, Applied Mathematics and Computation, **299** (2017), 66-79. https://doi.org/10.1016/j.amc.2016.11.039

[13] J. Lin, Y. Shi, S. Fei, Z. Gao, *Reliable dissipative control of discrete-time switched singular systems with mixed time delays and stochastic actuator failures*, IET Control Theory and Applications, **7**(11) (2013), 1447-1462. https://doi.org/https://doi.org/10.1049/iet-cta.2013.0028

[14] J. Liu, C. Wu, Z. Wang, L. Wu, *Reliable filter design for sensor networks using type-2 fuzzy framework*, IEEE Transactions on Industrial Informatics, **13**(4) (2017), 1742-1752. https://doi.org/10.1109/TII.2017.2654323

[15] S. Narayanamoorthy, S. P. Sathiyapriya, *A pertinent approach to solve nonlinear fuzzy integro-differential equations*, SpringerPlus, **5** (2016), 1-17. https://doi.org/10.1186/s40064-016-2045-4

[16] S. Narayanamoorthy, S. P. Sathiyapriya, *Homotopy perturbation method: A versatile tool to evaluate linear and nonlinear fuzzy Volterra integral equations of the second kind*, SpringerPlus, **5** (2016), 1-16. https://doi.org/10.1186/s40064-016-2038-3

[17] S. K. Nguang, W. Assawinchaichote, *H_∞ filtering for fuzzy dynamical systems with $\mathcal{D}$ stability constraints*, IEEE Transactions on Circuits and Systems-I: Fundamental Theory and Applications, **50**(11) (2003), 1503-1508. https://doi.org/10.1109/TCSI.2003.818624

[18] H. Peng, R. Lu, X. M. Li, S. Liu, *Reliable L_2-L_∞ filtering for fuzzy Markov stochastic systems with sensor failures and packet dropouts*, IET Control Theory and Applications, **11**(14) (2017), 2195-2203. https://doi.org/10.1049/iet-cta.2017.0361

[19] M. Sathishkumar, R. Sakthivel, F. Alzahrani, et al., *Mixed H_∞ and passivity-based resilient controller for nonhomogeneous Markov jump systems*, Nonlinear Analysis: Hybrid Systems, **34** (2019), 86-99. https://doi.org/10.1016/j.nahs.2018.08.003

[20] M. Sathishkumar, R. Sakthivel, O. M. Kwon, B. Kaviarasan, *Finite-time mixed H_∞ and passive filtering for Takagi-Sugeno fuzzy nonhomogeneous Markovian jump systems*, International Journal of Systems Science, **48**(7) (2017), 1416-1427. https://doi.org/10.1080/00207721.2016.1261199

[21] S. P. Sathiyapriya, C. Jana, N. Ivkovic, *Stability analysis of fuzzy generalized Abel integral equations using homotopy perturbation method*, European Journal of Pure and Applied Mathematics, **19**(1) (2026), 1-13. https://doi.org/10.29020/nybg.ejpam.v19i1.7059

[22] H. Shen, L. Su, J. H. Park, *Extended passive filtering for discrete-time singular Markov jump systems with time-varying delays*, Signal Processing, **128** (2016), 68-77. https://doi.org/10.1016/j.sigpro.2016.03.011

[23] Y. Shi, Y. Tang, S. Li, *Finite-time control for discrete time-varying systems with randomly occurring non-linearity and missing measurements*, IET Control Theory and Applications, **11** (2017), 838-845. https://doi.org/10.1049/iet-cta.2016.1367

[24] X. Su, P. Shi, L. Wu, Y. D. Song, *Fault detection filtering for nonlinear switched stochastic systems*, IEEE Transactions on Automatic Control, **61**(5) (2016), 1310-1315. https://doi.org/10.1109/TAC.2015.2465091

[25] X. Su, F. Xia, J. Liu, L. Wu, *Event-triggered fuzzy control of nonlinear systems with its application to inverted pendulum systems*, Automatica, **94** (2018), 236-248. https://doi.org/10.1016/j.automatica.2018.04.025

[26] Z. Sun, S. S. Ge, *Switched linear systems: Control and design*, Springer-Verlag, London, 2005. https://doi.org/10.1007/1-84628-131-8

[27] M. Syed Ali, et al., *Event-triggered H_∞ filtering for TS fuzzy discrete-time conic-type nonlinear networked control systems*, Iranian Journal of Fuzzy Systems, **21**(3) (2024), 137-154. https://doi.org/10.22111/ijfs.2024.46459.8184

[28] S. Wang, J. Feng, H. Zhang, *Robust fault tolerant control for a class of networked control systems with state delay and stochastic actuator failures*, International Journal of Adaptive Control and Signal Processing, **28**(9) (2014), 798-811. https://doi.org/10.1002/acs.2372

[29] J. Wang, S. Ma, C. Zhang, *Finite-time stabilization for nonlinear discrete-time singular Markov jump systems with piecewise-constant transition probabilities subject to average dwell time*, Journal of the Franklin Institute, **354**(5) (2017), 2102-2124. https://doi.org/10.1016/j.jfranklin.2017.01.014

[30] G. Wang, R. Xie, H. Zhang, et al., *Robust exponential H_∞ filtering for discrete-time switched fuzzy systems with time-varying delay*, Circuits, Systems, and Signal Processing, **35** (2016), 117-138. https://doi.org/10.1007/s00034-015-0062-0

[31] C. Wu, J. Liu, X. Jing, et al., *Adaptive fuzzy control for nonlinear networked control systems*, IEEE Transactions on Systems, Man, and Cybernetics: Systems, **47**(8) (2017), 2420-2430. https://doi.org/10.1109/TSMC.2017.2678760

[32] Z. G. Wu, J. H. Park, H. Su, et al., *Mixed $\mathcal{H}_\infty$ and passive filtering for singular systems with time delays*, Signal Processing, **93**(7) (2013), 1705-1711. https://doi.org/10.1016/j.sigpro.2013.01.003

[33] Y. Xia, J. He, H. K. Lam, et al., *Non-fragile fuzzy control of input-saturated systems with global prescribed performance via an error-triggered mechanism*, Information Sciences, **711** (2025), 122111. https://doi.org/10.1016/j.ins.2025.122111

[34] H. Yan, F. Qian, F. Yang, H. Shi, *H_∞ filtering for nonlinear networked systems with randomly occurring distributed delays, missing measurements and sensor saturation*, Information Sciences, **370-371**(6) (2015), 772-782. https://doi.org/10.1016/j.ins.2015.09.027

[35] H. Yang, P. Shi, X. Li, Z. Li, *Fault-tolerant control for a class of T-S fuzzy systems via delta operator approach*, Signal Processing, **98** (2014), 166-173. https://doi.org/10.1016/j.sigpro.2013.11.005

[36] S. Zhang, Z. Wang, D. Ding, et al., *Non-fragile H_∞ fuzzy filtering with randomly occurring gain variations and channel fadings*, IEEE Transactions on Fuzzy Systems, **24**(3) (2016), 505-518. https://doi.org/10.1109/TFUZZ.2015.2446509

[37] Y. Zhao, J. Wang, F. Yan, Y. Shen, *Adaptive sliding mode fault-tolerant control for type-2 fuzzy systems with distributed delays*, Information Sciences, **473** (2019), 227-238. https://doi.org/10.1016/j.ins.2018.09.002

[38] Q. Zheng, H. Zhang, *H_∞ filtering for a class of nonlinear switched systems with stable and unstable subsystems*, Signal Processing, **141**(C) (2017), 240-248. https://doi.org/10.1016/j.sigpro.2017.06.021